九州大学学術情報リポジトリ
Kyushu University Institutional Repository

Histidinylated poly-L-lysine based vectors for cancer-specific gene expression

趙, 國璽

https://doi.org/10.15017/1441065

出版情報：九州大学, 2013, 博士（工学）, 課程博士
バージョン：
権利関係：全文ファイル公表済

Histidinylated poly-L-lysine based vectors for cancer-specific gene expression

九州大学大学院

システム生命科学府

システム生命科学専攻

片山研究室

趙 國璽

目次

Chapter 1 Introduction 1
1-1 Background of Gene Therapy 1
1-2 Non-viral gene delivery pathway and the barriers 3
1-2-1 DNA complexation and cellular uptake 4
1-2-2 Endosomal escape 6
1-2-3 DNA release and nuclear entry 7
1-3 Cancer-targeting gene expression 8
1-3-1 Enhanced Permeability and Retention (EPR) effect 8
1-3-2 pH-responding system 10
1-3-3 Cell surface signaling-responding system 11
1-3-4 Intracellular signaling-responding system 11
1-4 Purpose of this research 13
1-5 Structure of this paper 14
1-6 Reference 15
Chapter 2 PLL-based pH and PKCα responding system 20
2-1 Introduction 20
2-1-1 Poly-amino acid based gene carrier 20
2-1-2 Protein kinase C (PKC) 21
2-1-3 Endosomal escape and buffering capacity 24
2-1-4 Design of this work 25
2-2 Result and discussion 25
2-2-1 Synthesis of the polymer 25
2-2-2 Protonation profiles of polymers 28
2-2-3 Ability of polymer to condense DNA at different pH 29
2-2-4 Cellular uptake of polyplex 31
2-2-5 *In vitro* cytotoxicity 32
2-2-6 *In vitro* transfection 34
2-2-7 Time-dependent gene expression 36
2-2-8 Intracellular distribution of polyplexes 37
2-3 Conclusion 39
2-4 Experiment Methods 40
2-5 Refenrence 47
Chapter 3 Akt-responding system with higher gene expression efficiency 51
3-1 Introduction 51

3-2 Protein kinase B (PKB, or Akt) 51
3-3 Results and discussion 55
3-3-1 Selection of Akt substrate 55
3-3-2 Balance of the cationic densities and endosomal escape moieties 57
3-3-3 Synthesis of Akt-responsive polymer 60
3-3-4 Coupled Enzyme Assay 62
3-3-5 Characterization of the polyplexes 64
3-3-6 Ethidium bromide Exclusion Assay 67
3-3-7 *In vitro* transfection 69
3-3-8 Influence of the Akt activity on gene expression 70
3-4 Conclusion 71
3-5 Experiment Methods 72
3-6 Reference 76
Chapter 4 Conclusion 78

Chapter 1 Introduction

1-1 Background of Gene Therapy

Comparing with the traditional drug-based therapy method, gene therapy provides a promising way to cure a disease at its source. Gene therapy was first conceptualized in 1972 by Theodore Friedmann and Richard Roblin[1]. The Human Genome Project (HGP) makes it possible to find disease-causing genes and use the information to develop more specific treatments. These years, there are many reports about the relationships between mutational gene and human diseases[2]. Because molecular mechanisms causing diseases by virulence genes have been clarified in many cases, gene therapy has been recognized as potentially promising medicine.

The first success of clinical trial in gene therapy was hold in 1990 by Dr. W. French Anderson[4]. The patient is a four-year old girl name Ashanti DeSilva, who lacked the enzyme adenosine deaminase (ADA) and suffered from an immune system dysfunction. Dr. Anderson's team drew blood from their patient and collected the leukocyte cells. After that, these cells were purified and transfected with ADA gene, and then injected back into her body. In this case, her body aquired the ability of ADA prodction and lead a normal life.

But accompanied with succeed gene therapy, there are also some serious medical accidents. In 1999, Jesse Gelsinger, an 18-year old boy, became the first patient who died from gene therapy[5]. He suffered from ornithine transcarbamylase deficiency, which lack the ability to metabolize ammonia. In this case, an adenoviral vector carrying a corrected gene was injected to test the safety of the procedure. This caused

serious immune response and lead to his death four days later. Other accidents occurred during X-SCID therapy in France[6] (2002) causing T cell leukemia. A patient, Jolee Mohr, also died in a rheumatic arthritis gene therapy (2007). Although Gelsinger's death is due to wrong operation and Mohr's death may be due to the massive fungal infection complicated[7], these accidents still made gene therapy fell into ice age. But gene therapy still has developed gradually. In 2009, the Science said "Gene Therapy Returns", by 2012, there are already 1771 clinical trials of gene therapy approved in the world[8]. It is necessary to treat gene therapy more carefully and find some safe way to deliver the therapeutic gene into target cells with low immunity and low toxicity.

To delivery therapeutic gene into target cells or tissues, two different strategies, *ex vivo* and *in vivo,* are performed (Fig. 1-1). As for the *ex vivo* method, target cells are modified *in vitro* by therapeutic gene, after multiplication, the cells containing therapeutic gene were transplanted into human body again. On the other hand, therapeutic gene are directly injected into human body for *in vivo* method with or without carrier and transfected into the cells for gene expression or suppression.

Ex vivo gene delivery is common and more certain, the transfected efficiency and targeting effect can be very high, and also the gene expression level could be controlled much easier than *in vivo* method. The problems which limit its application are mainly embodied in its requirement a mitotic cell population, a tissue culture method and a cell transplantation technology.

In the *in vivo* approach, the gene could be import into human body by simply injection. The gene may be delivered through a vector directly into the target cells or tissues. Comparing with ex *vivo method*, *in vivo* is more convenient and economical, and the application is more extensive. But low transfection efficiency and cytoxocity

also ailing the clinical application. In the application, virus vectors are used more common in the clinical, which take the percentage of more than 60% due to their easily preparation and high efficiency[8]. But considering of the safety, non-viral vectors attract more and more attention. This will be further discussed in 1-2 part.

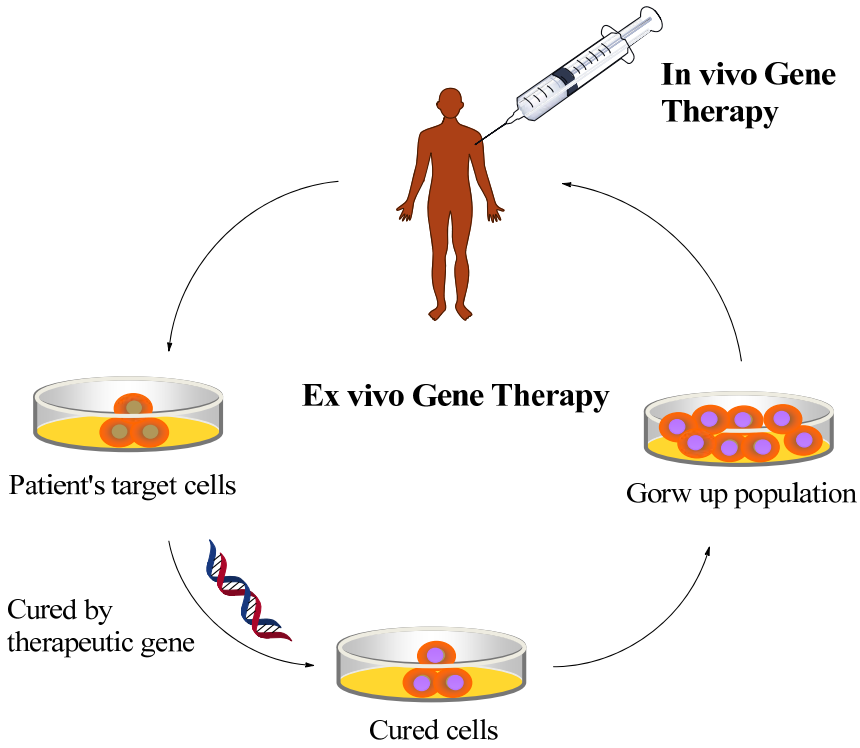

Figure 1-1: two kinds of gene therapy methods: In vivo and ex vivo

1-2 Non-viral gene delivery pathway and the barriers

As described above, non-viral gene therapy has been widely studied. In this division, I will introduce the generally accepted gene therapy pathway and some methods to overcome the barriers in gene delivery.

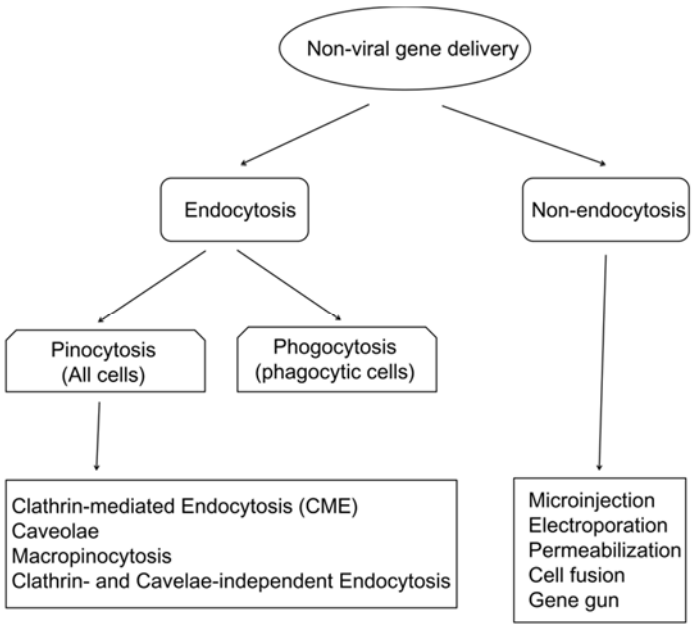

Figure 1-2: Different cellular uptake pathway in non-viral gene delivery

1-2-1 DNA complexation and cellular uptake

The cellular uptake pathway of gene delivery with non-viral vectors is shown in Fig. 1-2. It could be classified into endocytosis and non-endocytosis pathways. The non-endocytosis cellular uptake, such as electroporation method、"gene gun" or microinjection, use chemical or physical methods to transfect foreign gene into target cells. These methods could be quite efficient, but they are not so feasible. In most situations, these methods are not suitable, especially in clinical application. In contrast, the endocytosis cellular uptake provides a more facile way for gene transfection. Clathrin-mediated endocytosis (CME) is the major pathway[9-10] of endocytosis (Fig. 1-3). In a brief, the ligand firstly binds to the cell surface by electrostatic interaction or specific cell surface receptor. After that, the clathrin, AP-2 adaptor, AP180, actin and other components are assembled and formed coated pits. Finally, the coated pits mature and pinch off from the plasma membrane, resulting in an early endosomes and transition towards the cytoplasm.

Because the cellular uptake of free DNA is hindered by the big size and negative charge of the DNA, gene carriers are generally employed to condense DNA into proper size for an efficient cellular uptake. In these methods, the binding of polymer/DNA complexes (polyplexes) or (liposome/DNA complexess) lipoplexes to the cell surface is generally by the nonspecific ionic interaction between the positive charged complexes and negative charged cell surface. Many researchers have revealed that size[33, 34] and surface charge[35] of complexes govern the cell uptake process. The complexes with a diameter of <200 nm are generally uptaken via CME process, whereas caveolae-mediated internalization became pre-dominant with increasing particle size[36]. Furthermore, the complex surface functionality also plays an important role in cellular uptake. The gene carrier modified by some ligands which can be specially recognized by the cell surface receptor, such as transferrin, could increase the cellular uptake[12], so as to increase the transfection efficiency. There are also some reports that the modification of HIV-Tat, a cell-penetrating peptide, could increase the cellular uptake efficiently [61].

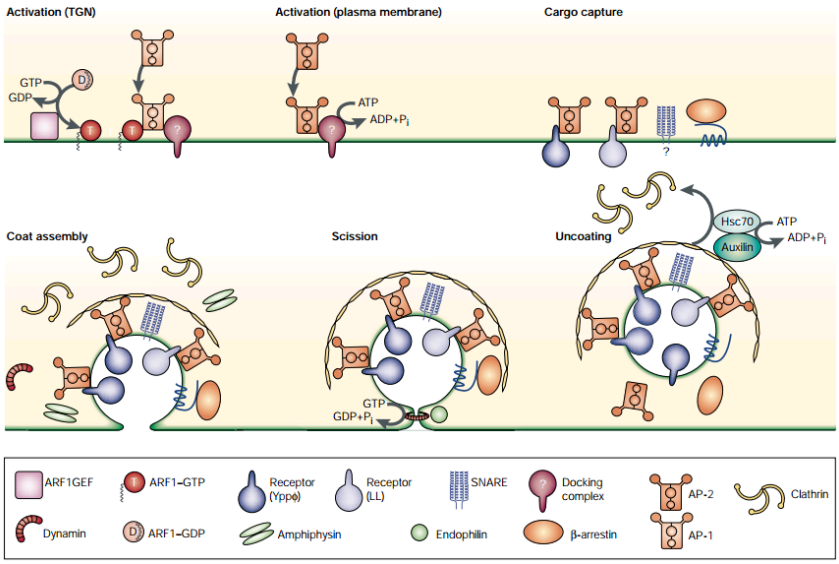

Figure 1-3: the key steps of CME[11]

1-2-2 Endosomal escape

After entering the cells by endocytosis, the complex is located in the endosome. After that, along with the decrease of inside pH, the endosome will fuse with lysosome for degradation of encapsulated molecules or recycle the receptors back to the cell membrane. In this case, endosomal escaping ability of the gene/carrier complex is necessary for high efficient gene expression.

In the case of lipoplexes, liposome could fuse with the membrane of endosome, so as to release the transfected DNA to the cytosol[13, 14]. In the case of polyplexes, the endosomal escaping is generally considered to be due to the buffering capacity of the polymer. This hypothesis was first suggested by Behr et al using Polyethylenimine (PEI) [15]. During the maturation step from early endosome to late endosome, the pH will decrease from pH = 7.4 to about 5.5. Polyethylenimine (PEI) is a typical polymer that has good buffering capacity at endosomal pH range. The hypothesis suggests that at the lower pH, PEI becomes more protonated. This protonation causes the protons and Cl^-

pumped into the endosome, following the increase of water influx and finally causing the swelling and rupturing of the endosomes (Fig.1-4). This effect based on the buffering capacity between pH 7.4 ~ 6.5 is so called "proton sponge effect". Because of this ability, PEI shows higher gene transfection efficiency comparing with other polycations. Other molecules such as chloroquine[16], morpholine[62], imidazole[63] and histidine[64] with proton sponge ability are also used for the endosomal escape. But recently there are also some debates about this interpretation[65]. Based on this hypothesis, lowering of the pH in endosome and lysosome should be suppressed due to the buffering effect. Andresen et al. reported that this incensement cannot be detected, and it is doubt whether proton sponge effect is the dominant mechanism of polyplex escape.

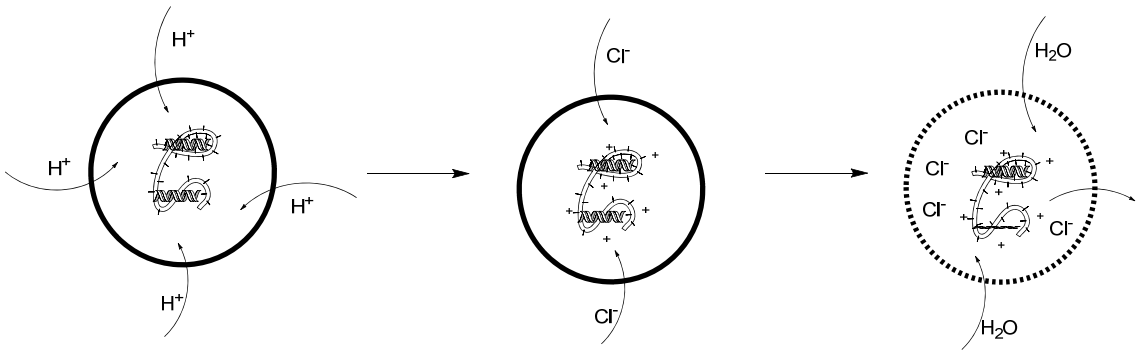

Figure 1-4: Endosomal escape by buffering capacity

1-2-3 DNA release and nuclear entry

After the complexes escape from the endosome, the DNA need to be released and transferred into nuclear for transcription[66]. Polymers which can change its property responding to the intracellular environment can induce DNA release. For example, polymers with functional bonds degradable at acidic pH in the endolysosomes, can form a stable polyplex with DNA in the extracellular environment. In the intracellular environments, the acid-triggering degradation of these polymers release the DNA into

cytosol[17].

The nuclear membrane contains nuclear pores with a diameter of about 10 nm and applys a passive transport of molecules less than 70 kDa [18]. Molecules more than 45 kDa require specific targeting signals to gain either access to or egress from the nucleus[19]. There are some reports about coupling nuclear localization signal (NLS) to the transfected DNA to increase the gene expression level [20-22].

1-3 Cancer-targeting gene expression

As mentioned in 1-1, viral vectors are more efficient than non-viral vectors, but the safety and confidence are the problems. Therefore, despite the low efficiency comparing with viral vectors, non-viral vectors attract a great deal of interest due to their advantageous safety profile. But how to deliver the foreign gene into target cells is also critical for non-viral gene therapy, especially for the cancer therapy for which the therapeutic genes are generally toxic and would otherwise kill the transfected cell. In this section, we will introduce some methods for targeting gene therapy to secure cell specificity.

1-3-1 Enhanced Permeability and Retention (EPR) effect

EPR effect was first conceptualized in 1986 by Mathumura and Maeda[35], which means the certain sizes of molecules tend to accumulate in tumor tissues much easier than they do in normal tissues (Fig. 1-5). The general explaination is that, in tumor tissues, the newly formed blood vessels are usually accompanied by discontinuity within the vascular endothelial layer due to the sustain rapid growth and abnormal growth factors. Studies indicate the mean pore size of most peripheral human tumors is in the range from 200 nm to 600 nm in diameter[36]. Comparing with normal vessels,

these tumor vessels have gaps of several hundred nanometers among the cells. Furthermore, tumor tissues usually lack effective lymphatic drainage so that the excretion of high molecules are more difficult. In this case, for molecules with diameter between dozens of nanometers and hundreds of nanometers, the permeability and retention in tumor tissues are much easier that in normal tissues.

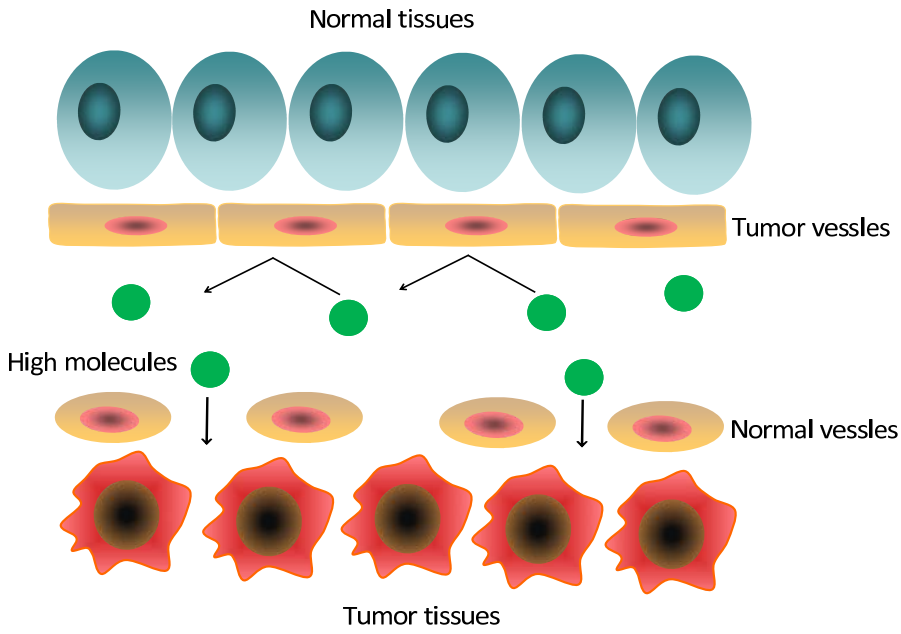

EPR effect is utilized for cancer specific delivery of many macromolecular systems. Thus high molecules with long circulation time in blood will be able to extravasate more efficiently through the vasculature and accumulate in the tumor tissues. To achieve this, Polyethylene glycol (PEG) is generally used for chemical modification of various carriers to make them more stable and long- circulating[67]. Another strategy is the utilization of NO-releasing agents such as nitroglycerin, which could releases nitrite. Nitrite is converted to NO in the tumor tissues, which leads to a significantly increased EPR effect and enhanced antitumor drug effects as well[68].

1-3-2 pH-responding system

The environmental pH of turmors is generally lower than that of the normal tissues. The pH of normal tissues is about 7.4, whereas the pH of turmer lesions is about 6.5 [40]. This is because of the unregulated proliferation of cancer cells. While the tumor mass increases, the interior of the tumor grows farther away from existing blood supply. So the cancer cells are generally oxygen-deficient, and the produced lactic acid due to the anaerobic respiration reduced the microenvironment pH. Take advantage of this, many kinds of pH-responsive carriers have been developped. For example, poly(β-amino ester) (PbAE, Fig. 1-6a) is a pH-sentisive cationic polymer and undergoes rapid dissolution when the pH of the medium is less than 6.5 [39]. D. Shenoy et al. have reported that this polymer showed rapid dissolution and elimination, and released its contents within the acidic tumor microenvironment and endo/lysosome compartments of cells. Our laboratory also developed a branched poly- ethyleneimine (bPEI) based pH-sensitive polymer[37] (Fig. 1-6b). This polymer was obtained by modifying polyethylene glycol (PEG) onto branched polyethyleneimine (bPEI) through an acid labile linker. The polymer could release the PEG chains under the slightly acidic extracellular pH associated with cancer cells, so as to achieve both stability in physiological conditions and efficient cellular uptake in solid tumors.

(a)

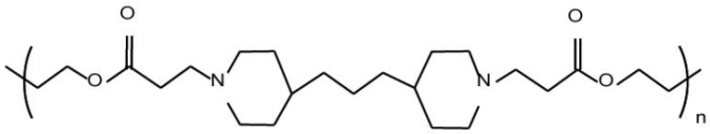

(b)

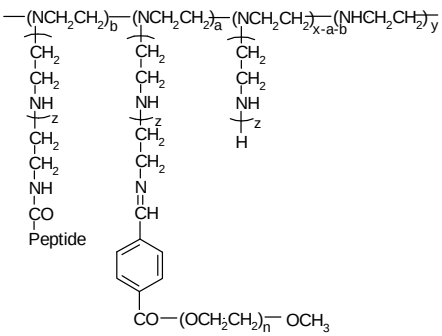

Figure 1-6: The chemical structure of (a) representative hydrophobic poly(β-amino ester) (PbAE) and (b) bPEI-based protein kinase- and acidosis-responsive gene carrier

1-3-3 Cell surface signaling-responding system

Cancer cells employ mechanisms for hyper-proliferation and to bypass these safeguards, including increased signaling for cell growth, evasion of cell death and increased blood vessel formation. All these mechanisms are concern with the abnormal cell signaling pathway and one of the direct results is the overexpression of some kinds of cell surface receptors, including epidermal growth factor receptors (EGFR) [41, 42], folate receptors (FR) [43], transferrin receptors[44] or others[45]. The gene carriers modified with ligands that can specifically bind to these surface receptors, have been wildly utilized for cancer cells specific gene delivery[46-50]. However, the method is suffered from heterogeneity of tumor tissue and expression of such receptors in normal cells.

1-3-4 Intracellular signaling-responding system

In contrast to cell surface signaling, intracellular signaling is another promising

target to recognize disease cell from normal cell. The cell signaling pathway is important for cell responding to environment stimulation, and the disrupted pathway will cause unregulated cell proliferation, migration, apoptosis, and differentiation. The protein kinases and proteinase play very important role in this signaling pathway, comprising receptor tyrosine kinases (RTKs) such as EGFR, HER2, ALK, and ROS1 and their corresponding downstream signaling targets, including Akt, MAPK, and others. In cancer cells, generally some kinds of certain cell signaling are hyper-expressed[51-54]. Thus, these hyper-activated cell signaling could also be targeted for cancer cell selective gene expression.

Responding to the hyper-activated intracellular signaling, our laboratory has developed a specific drug or gene release system, which is called "Drug- or Gene-delivery system responding to cellular signals" (D-RECS) (Fig. 1-6). This D-RECS uses hyper-activated signals as a trigger to release the gene from the carrier and thus to activate gene expression. Many kinds of protein kinase or protease are hyper-expressed in different kinds and stages of cancers, so this method is expected to be applicable to any protein kinases that are activated specifically in different cancers. Until now, we have already succeed in PKA[55-56]、PKCα[57–58]、ROCK[59] and caspase[60] responding gene expression.

A polymeric D-RECS carrier generally contains two parts: polymer based main chain and cationic charged substrate peptide pendant chain. This totally cationic charged polymer could condense DNA into polyplex by electrostatic interaction. In normal cells, this polyplex could be stable, and the transfected DNA will not be released. But in target cells, this substrate peptide will be phosphorylated by the hyper-activated protein kinase, leading to a neutralization of the cationic net charge. Thus the DNA will be

released, and activate the gene transcription.

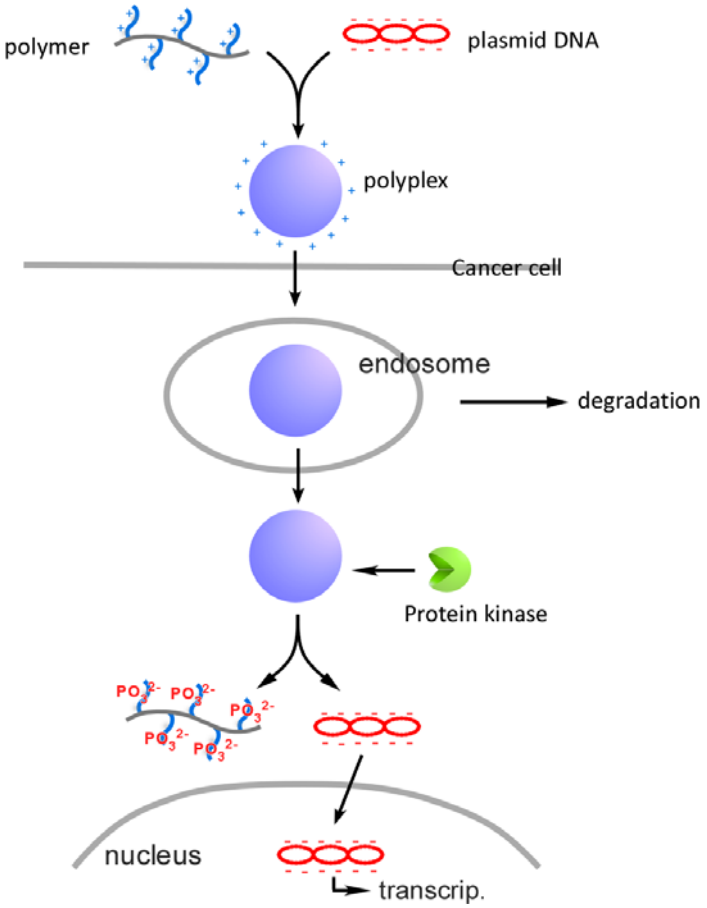

Figure 1-6: Concept of D-RECS

1-4 Purpose of this research

As described above, comparing with virus vectors, non-viral vectors attract more and more attention because of their safety. But the low efficiency limits their application. Furthermore, reducing the side-effect due to the activation of delivered gene in non-target cells is still one of the most important problems. This is especially critial for the cancer disease, in which the therapeutic genes are generally toxic and would cause the transfected cell death. In this work, we design a safe and high efficient gene carrier and tried to overcome these disadvantages. This work is based on D-RECS strategy, and

devote to design a more easily prepared and more efficient gene carrier.

1-5 Structure of this paper

This paper is composed by 4 chapters. In the chapter 2, based on our previous work, we developed a new easily-synthesized polymer, which can be used as a high efficient and cancer-cell-targeted gene carrier, based on the intracellular signaling – protein kinase Cα (PKCα). In the chapter 3, we further studied these polymers and tried to balance the cationic centers and endosomal escape moieties. These polymers were also be applied to another protein kinase to enlarge the application range of this system. Chapter 4 is the conclusion and further expectation.

1-6 Reference

1. Theodore Friedmann, Richard Roblin, *Science* **1972**, 175, 949-955
2. http://en.wikipedia.org/wiki/List_of_genetic_disorders
3. Eliot Marshall, *Science* **1999**, 286, 2244-2245
4. http://www.lifesciencesfoundation.org/printer_events-The_first_gene_therapy.html
5. http://en.wikipedia.org/wiki/Jesse_Gelsinger
6. Bernd Gansbacher President, *J. Gene Med.* **2003**, 5,261-262
7. Meredith Wadman, *Nature* **2007**, 449, 270
8. http://www.wiley.com//legacy/wileychi/genmed/clinical/
9. Christophe Lamaze, Sandra L Schmid, *Curr. Opin. Cell Biology* **1995**, 7, 573-580
10. Kohji Takei, Volker Haucke, *Trends in Cell Biology*, **2001**, 11, 385-391
11. Tomas Kirchhausen, *Nature Reviews Molecular Cell Biology,* **2000**, 1, 187-198
12. Willem Stoorvogel, Ger J. Strous, Hans J. Geuze, Viola Oorschot, Alan L. Schwartzt, *Cell*, **1991**, 65, 417-427
13. Hassan Farhood, Natalya Serbina, Leaf Huang, *Biochimica et Biophysica Acta (BBA) – Biomembranes*, **1995**, 1235, 289-295
14. J P Behr, B Demeneix, J P Loeffler, and J Perez-Mutul, *PNAS*, **1989**, 86, 6982-6986
15. O Boussif, F Lezoualc'h, M A Zanta, M D Mergny, D Scherman, B Demeneix, and J P Behr, *PNAS*, **1995**, 92, 7297-7301
16. Tomoyuki Kakudo, Shinji Chaki, Shiroh Futaki, Ikuhiko Nakase, Kenichi Akaji , Toru Kawakami, Kazuo Maruyama, Hiroyuki Kamiya and Hideyoshi Harashima, *Biochemistry*, **2004**, 43, 5618–5628
17. Christopher L. Grigsby and Kam W. Leong, *Interface Focus*, **2011**, 6, 702-724
18. F Melchior, T Guan, N Yokoyama, T Nishimoto, and L Gerace, *J. Cell Biol.*, **1995**, 131, 571-581

19. Kylie M. Wagstaff, David A. Jans, *Eur. J. Pha*., **2009**, 625, 174-180

20. Jans DA and Hubner S, *Physiol Rev*, **1996**, 76, 651-685

21. Magdolna G. Sebestyén, James J. Ludtke, Michael C. Bassik, Guofeng Zhang, Vladimir Budker, Eugeny A. Lukhtanov, James E. Hagstrom & Jon A. Wolff, *Nature Biotechnology*, 1998, 16, 80 - 85

22. Alexander G. Tkachenko, Huan Xie, Donna Coleman, Wilhelm Glomm, Joeph Ryan, Miles F. Anderson, Stefan Franzen, and Daniel L. Feldheim, *J. Am. Chem. Soc*., **2003**, 125, 4700–4701

23. JA Wolff, RW Malone, P Williams, W Chong, G Acsadi, A Jani, PL Felgner, *Science*, **1990**, 247, 1465-1468

24. Young K. Song, Feng Liu, Shaoyou Chu and Dexi Liu, *Human Gene Therapy*. **1997**, 8, 1585-1594

25. Ogris M, Brunner S, Schüller S, Kircheis R, Wagner E, *Gene Therapy*, **1999**, 6 595-605

26. M. D. Brown, A. Schätzlein, A. Brownlie, V. Jack, W. Wang, L. Tetley, A. I. Gray, and I. F. Uchegbu, *Bioconjugate Chem.*, **2000**, 11, 880–891

27. M. Anne Hickman, Robert W. Malone, Karin Lehmann-Bruinsma, Tracey R. Sih, Daren Knoell, Francis C. Szoka, Rosemary Walzem, Don M. Carlson and Jerry S. Powell, *Human Gene Therapy*, **1994**, 5, 1477-1483

28. Yang JP and Huang L, *Gene Therapy*, **1996**, 3,542-548

29. Wei Hong Yu, Mohammed Kashani-Sabet, Denny Liggitt, Dan Moore, Timothy D Heath and Robert J Debs, *J. Investigative Dermatology*, **1999**, 112, 370-375

30. Jim Haralambidis, Lucy Duncan, Geoffrey W. Tregear, *Tetrahedron Lett.*, **1987**, 28, 5199-5202

31. Jean-Christophe Truffert, Olivier Lorthioir, Ulysse Asseline, Nguyen T. Thuong, André Brack, *Tetrahedron Lett.*, **1994**, 35, 2353-2356

32. Ramon Eritja, Anna Pons, Mónica Escarcellar, Ernest Giralt, Fernando Albericio, *Tetrahedron Lett.*, **1991**, 47, 4113-4120

33. B. Devika Chithrani, Arezou A. Ghazani, and Warren C. W. Chan, *Nano Lett.,* **2006**, 6, 662–668

34. Carl D. Walkey, Jonathan B. Olsen, Hongbo Guo, Andrew Emili, and Warren C. W. Chan, *J. Am. Chem. Soc.* **2012**, 134, 2139–2147

35. Mathumura,y.; Maeda,H. *Cancer Res.* **1984**,46,6387-6392

36. Yuan, F., Dellian, M., Fukumura, D., Leunig, M., Berk, D. A., Torchilin, V. P., and Jain, R. K. *Cancer Res.*, **1995**, 55, 3752-3756

37. Satoshi Kushio, Akira Tsuchiya, Yuta Nakamura, Takanobu Nobori, Chan Woo Kim, Guo Xi Zhao, Taiki Funamoto, Eun Kyung Lee, Takuro Niidome, Takeshi Mori, Yoshiki Katayama, Biomed. Eng. Appl. Basis Commun., **2013**, 25

38. Oh, K.T.; Baik, H.J.; Lee, A.H.; Oh, Y.T.; Youn, Y.S.; Lee, E.S. *Int. J. Mol. Sci.* **2009**, *10*, 3776-3792.

39. D. Shenoy, S. Little, R. Langer, M. Amiji, *Mol. Pharmacol.* **2005**, 2, 357-366

40. Ian F. Tannock, Daniela Hotin, Acid pH in Tumors and Its Potential for Therapeutic Exploitation, *Caner Research*, **1989**, 49, 4373-4384

41. S.H. Torp, E. Helseth, A. Dalen, G. Unsgaard, *Cancer Immunol. Immunother.* **1991**, 33, 61–64.

42. V. Rusch, J. Mendelsohn, E. Dmitrovsky, *Cytokine Growth Factor Rev*. **1996**, 7, 133–141

43. S.D. Weitman, R.H. Lark, L.R. Coney, D.W. Fort, V. Frasca, V.R. Zurawski Jr., B.A. Kamen, *Cancer Res.* **1992**, 52, 3396–3401.

44. L. Recht, C.O. Torres, T.W. Smith, V. Raso, T.W. Griffin, *J. Neurosurg.* **1990**, 72, 941–945.

45. B.J. Simpson, H.A. Phillips, A.M. Lessells, S.P. Langdon, W.R.Miller, *Int. J. Cancer* **1995**, 64, 202–206.

46. Anatoly N. Lukyanov, Tamer A. Elbayoumi, Ananthsrinivas R. Chakilam, Vladimir P. Torchilin, *J. Controlled Release*, **2004**, 100, 134-144

47. Hyuk Sang Yoo, Tae Gwan Park, *J. Controlled Release*, **2004**, 96, 273-283

48. Ying Xie, Liya Ye, Xiaobin Zhang, Wei Cui, Jinning Lou, Tsuneji Nagai, Xinpu Hou, *J. Controlled Release*, **2005**, 105, 106-119

49. David A. Eavarone, Xiaojun Yu, Ravi V. Bellamkonda, *J. Biomedical Materials Research*, **2000**, 51, 10-14

50. Christopher P. Leamon , Scott R. Cooper and Gregory E. Hardee, *Bioconjugate Chem.*, **2003**, 14, 738–747

51. Rayudu Gopalakrishna, Susan Jaken *Free Radical Bio. Med.*, **2000**, 28, 1349-1361

52. Jeremy R. Graff, et al, *J. Biol. Chem.* **2000**,275, 24500-24505

53. Kim S. H., Forman A. P., Mathews M. B. and Gunnerys. *Oncogene* **2000**, 19, 3086-3094

54. David T. Price, Gregory Della Rocca, ChuanHai Guo, Michael S. Ballo, Debra A. Schwinn, Louis M. Luttrell, *J.Urol.*, **1999**, 162, 1537-1542

55. Tatsuhiko Sonoda, Takashi Nogami, Jun Oishi, Masaharu Murata, Takuro Niidome and Yoshiki Katayama, *Bioconjug. Chem.*, **2005**, 16, 1542-1546

56. Jun Oishi, Kenji Kawamura, Jeong-Hun Kang, Kota Kodama, Tatsuhiko Sonoda, Masaharu Murata, Takuro Niidome, Yoshiki Katayama, *J.Control. Release*, **2006**, 110, 431-436

57. Jeong-Hun Kang, Daisuke Asai, Jong-Hwan Kim, Takeshi Mori, Riki Toita, Tetsuro Tomiyama, Yoji Asami, Jun Oishi, Yuko T. Sato, Takuro Niidome, Byungdug Jun , Hideki Nakashima and Yoshiki Katayama, *J. Am. Chem. Soc.*, **2008**, 130, 14906-14907

58. Riki Toita, Jeong-Hun Kang, Tetsuro Tomiyama, Chan Woo Kim, Shujiro Shiosaki, Takuro Niidome, Takeshi Mori, and Yoshiki Katayama, *J. Am. Chem. Soc.*, **2012**, 134, 15410-15417

59. Akira Tsuchiya, Jeong-Hun Kang, Daisuke Asai, Takeshi Mori, Takuro Niidomea, Yoshiki Katayama, *J. Am. Chem. Soc.*, **2011**, 155, 40-46

60. Kenji Kawamura, Jun Oishi, Jeong-Hun Kang, Kota Kodama, Tatsuhiko Sonoda, Masaharu Murata, Takuro Niidome, and Yoshiki Katayama, *Biomacromolecules*, **2005**, 6, 908-913

61. M. Mae, U. Langel, *Curr. Opin. Pharmacol.*, **2006**, 6, 509-514

62. S. Fukushima, K. Miyake, N. Nishiyama, N. Kanayama, Y. Yamasaki, K. Kataoka, *J. Am. Chem. Soc.*, **2005**, 127, 2810-2811

63. David Putnam, Christine A. Gentry, Daniel W. Pack, and Robert Langer *Proc. Natl.Acad. Sci. USA* **2001**, 98, 1200-1205

64. Patrick Midoux and Michel Monsigny *Bioconjugate Chem.* **1999**, *10,* 406-411

65. Rikke V Benjaminsen, *Molecular Therapy*, **2013**, 21, 149-157

66. K. M. Wagstaff, D. A. Jans, *Eur. J. Pharm.*, **2009**, 625, 174-180

67. Duncan, R. *Nat. Rev. Drug Discovery*, **2003**, 2, 347-360

68. Fang J, Nakamura H, Maeda H. *Adv Drug Deliv Rev.* **2011**, 63,136-151

Chapter 2 PLL-based pH and PKCα responding system

2-1 Introduction

As described in chapter 1, our group has developed a gene delivery system called D-RECS (Drug- or Gene- delivery systems responding to cellular signals). Based on this strategy, we have developed several kinds of polymers whose main chain is based on polyacrylamide [1-5] or polyethyleneimine (PEI) [6, 7]. These polymers showed cancer-cell-specific gene expression ability, but either the difficulty in controlling the polymer's molecular weight or the troublesome synthetic procedures may limit their application. Furthermore, both of the two polymers are not biodegradable.

To overcome these problems, we used poly-L-lysine (PLL) as a new D-RECS main chain. The synthesis of this carrier was straightforward, proceeding via the modification of side-group-protected substrate peptide and protected histidine followed by their deprotection. In this chapter, we will introduce this polymer.

2-1-1 Poly-amino acid based gene carrier

Composed of essential amino acid, poly-amino acid generally can be degraded by enzymes into monomer. These carriers have good biocompatibility and no immunogenicity. Poly-Aspartic acid (PAA), poly-glutamic acid (PGA), poly-l-lysine (PLL), poly-histidine, poly-alanine and poly-phenylalanine are widely studied as gene carrier.

Poly-L-lysine (PLL) is a well-known polymeric gene carrier. At neutral pH, each of the amino acid residues contains one positive charge, which makes PLL be able to strongly interact with plasmid DNA (pDNA) and condense pDNA to a proper size for

cellular uptake [8]. However, because PLL tends to over-condense and cannot escape from the endosome, its use tends to yield relatively poor gene expression [9, 10]. Polylysine is used commercially as a safely food preservative, but the cytotoxicity of PLL as gene carrier cannot be neglected. This is because of the high charge density makes it adsorbed electrostatically to the cell surface and causes cell death. This disadvantage also presents problems for its use as a polymeric gene carrier.

2-1-2 Protein kinase C (PKC)

As described in chapter 1, in many kinds of cancer cells, certain protein kinases are hyper-expressed and activated. In this study, we focus on PKCα, which is one of the most studied target kinase in our group.

PKCα is a superfamily of serine/threonine kinases and plays an important role in several signal transduction cascades, and could be activated by phosphatidylserine (PS) and diacylglycerol (DAG) in a Ca^{2+}-dependent manner. PKC superfamily has more than 10 members[11, 12]. According to their structure, they could be subdivided into conventional PKC (cPKC), novel PKC (nPKC) and atypical PKC (aPKC) isoforms (Fig. 2-1). PKCα is a kind of cPKC isoform and is one of the first isotypes to be identified and cloned.

All of these PKC isoforms contain a highly conserved kinase domain (catalytic domain) at C-terminal, and a regulatiory domain at N- terminal, in which most of the structural differences reside. The regulatory domain generally contains three functional elements: (i) an inhibitory region (pseudosubstrate), (ii) a zinc finger or C1 domain and (iii) a C2 domain. The C1 domain, present in all of the isoforms of PKC, has one or two repeated zincfinger motifs. It has a binding site for DAG as well as non-hydrolysable,

non-physiological analogues called phorbol esters. The aPKCs contain a single zinc finger motif, and are not responsive to phorbol esters. The function of the single zinc finger of aPKCs is not quite clear. The C2 domain, present in both cPKCs and nPKCs, acts as a Ca^{2+} sensor. It could bind to phospholipid vesicles in a Ca^{2+}-dependent manner. The pseudosubstrate (PS) region is present in all three isoforms of PKC. This is a small sequence of amino acids that mimic a substrate and interacts with the catalytic domain, and is responsible for the intramolecular suppression of catalytic activity prior to effector binding. When the Ca^{2+} and DAG present in sufficient concentrations, they binds to the C2 and C1 domain and recruit PKC to the membrane [13, 14]. This interaction with the membrane results in release of the PS from the catalytic site and activation of the enzyme.

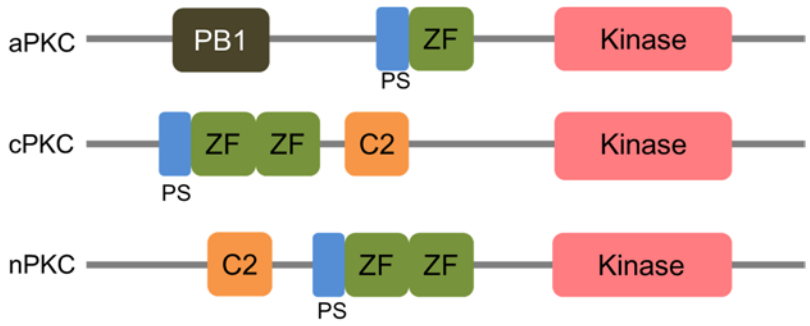

Figure 2-1: Structure of different PKC subfamily. aPKC: atypical PKC; cPKC: classical PKC; nPKC: novel PKC. PB1: PB1 dimerization domain; PS: pseudosubstrate region; ZF: zinc finger; C2: C2 domain; Par-4: partitionindefective 4

Activated by tumor promoter phorbol ester, PKCα may phosphorylate downstream transcription activators. This will lead to increased expression of oncogenes, promoting cancer progression, including proliferation, intravasation and metastasis[15]. The disorder

of PKCα has been confirmed in various kinds of cancer cells. For example, the hyper-activated PKCα has been detected in cutaneum cancer[16-18], colorectal cancer[19], prostatic cancer[20], breast cancer[21, 22], lung cancer[23] and liver cancer[24, 25]. Therefore, PKCα targeting gene therapy could be a promising method for cancer therapy.

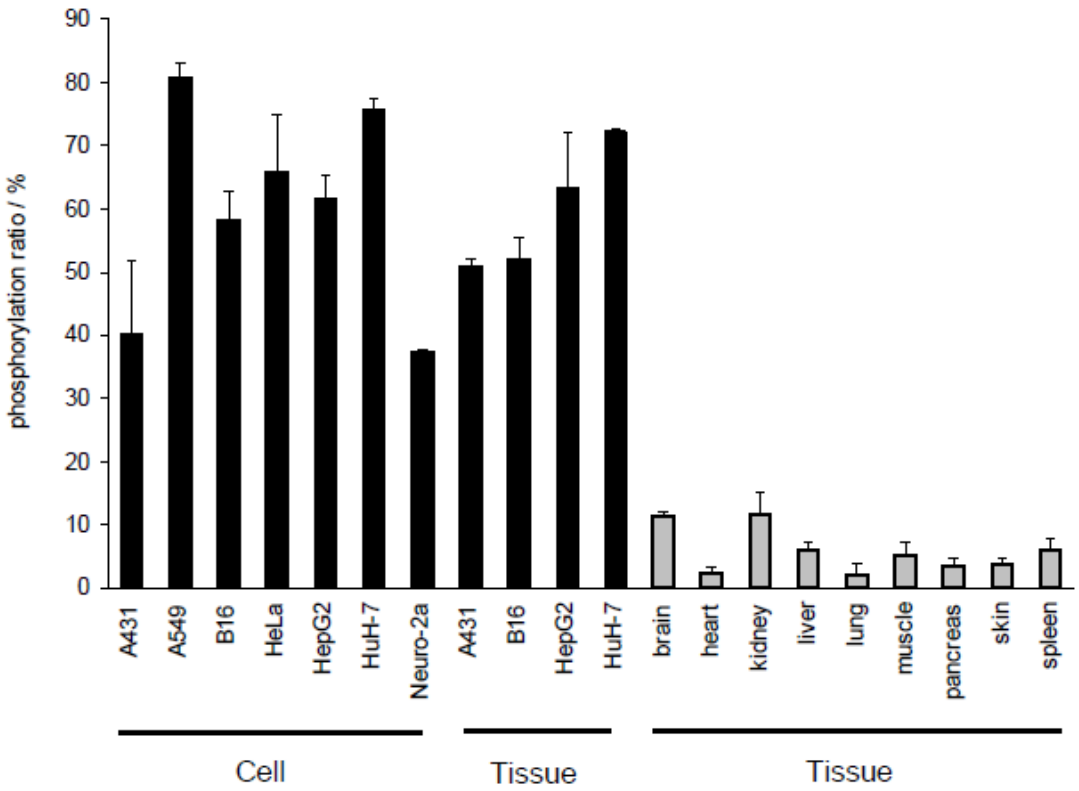

Figure 2-2: PKCα activity of different kinds of cells and tissues[26].

To design a D-RECS polymer, the specific substrate for hyper-activated protein kinase is one of the most important parts. By using Scansite data, our laboratory found a substrate peptide showing high specificity for PKCα relative to other isozymes. This peptide was named Alphatomega (H-FKKQGSFAKKK-NH_2). The Km and Vmax of this peptide is shown in Tab. 2-1. In this experiment, we also chose this sequence as PKCα specific substrate peptide. According to this property, Alphatomega showed high

specificity to various cancer cells comparing with other normal tissues (Fig. 2-2).

Table 2-1: Kinetic parameters (Km, Vmax, and Vmax/Km) for Alphatomega[26]

Isozymes	K_m (μM)	V_{max} (nmol/min/mg)	V_{max}/K_m
α	17.4	138	7.9
βI	35.6	175	4.9
βII	59.9	38.6	0.6
γ	34.7	47.0	1.4
δ	42.2	8.8	0.2
ε	22.9	66.2	2.9
η	16.6	41.8	2.5
θ	34.0	7.6	0.2
ζ	20.5	17.4	0.9
ι/λ	25.8	90.4	3.5

2-1-3 Endosomal escape and buffering capacity

In chapter 1-2-1, I described the endosomal escape barrier of gene transfection. The endocytic pathway is the major uptake mechanism of cells, and how to release the cargo from endosome is one of the main limiting steps in effective biological based therapy. To facilitate the endosomal escape, many mechanisms have been introduced, for example, pore formation in the endosomal membrane, fusion into the lipid bilayer of endosomes and buffering capacity of weak base groups.

As mentioned in 2-1-1, PLL has high cationic charges at neutral pH. Lack of endosomal escape ability limits its application. To solve this problem, researchers have converted the ε-amine group of PLL to weak basic groups such as imidazole, histidine, and ornithine [27-33]. These basic groups provide the resulting polymer with buffering capacity at endosomal pH, and decrease its cationic charge density compared with that of PLL to reduce the cytotoxicity [10].

2-1-4 Design of this work

In this work, we employed PLL as main chain for its easily modifiable property. PKCα substrate peptide and histidine were then modified onto this main chain, respectively. The peptide group is designed to work as phosphorylation motif and cationic charge motif. The histidine group is to work as buffering motif and to reduce the cytotoxicity of PLL main chain.

2-2 Result and discussion

2-2-1 Synthesis of the polymer

Modification of polymers with peptides is often troublesome because of side reactions. In this work, the polymer synthesis is facile and straightforward, based on the reaction of a protected peptide in organic solvent. First, the primary amines of the PLL were modified with side-group-protected peptides and Fmoc-His(Trt). Next, the protecting groups were removed to obtain the final product (Scheme 2-1). The sequence of peptide used here was FKKQGSFAKKK-NH_2, which is a specific substrate of the target protein kinase, PKCα [26]. We also prepared a negative control polymer (PA-H) carrying a non-reactive peptide, FKKQGAFAKKK-NH_2, in which the serine residue was relaced with alanine. The histidine-unmodified polymers (PS, PA) and peptide-unmodified polymer (P-H) were also prepared as controls. Table 2-2 summarizes the peptide and histidine content of the synthesized polymers. These contents were calculated from the ^{1}H NMR spectral signals (Figure 2-3b) at $\delta = 7.88$ ppm (the imidazole moiety in the histidine), $\delta = 7.23$ ppm (the benzene moiety in the peptide phenylalanine), and $\delta = 4.14$ ppm (the α-CH moiety in the PLL main chain).

Because our gene delivery system is sensitive to the charge shift of the grafted peptide upon phosphorylation, the high histidine ratio will both increase the buffering capacity and minimize the contribution of the cationic PLL main chain on the polyplex formation.

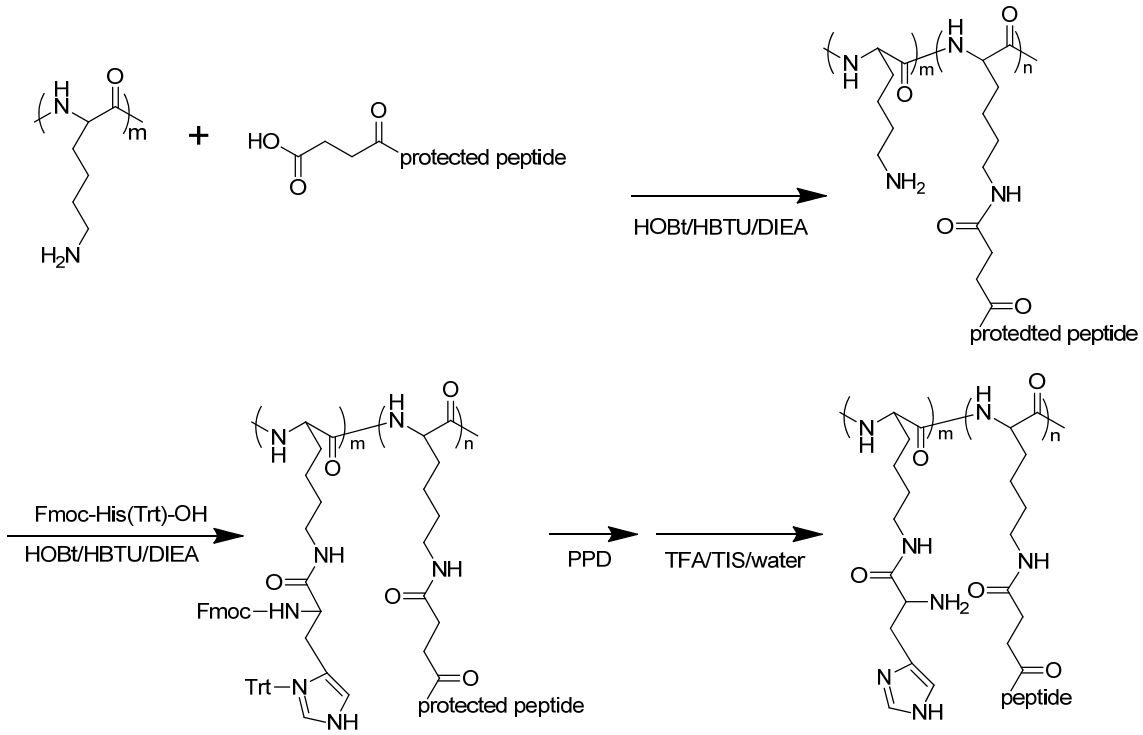

Scheme 2-1. Synthesis of histidine- and peptide-modified PLL (PS-H and PA-H). Peptide = -FKKQG<u>S</u>FAKKK-NH_2 or -FKKQG<u>A</u>FAKKK-NH_2

(a)

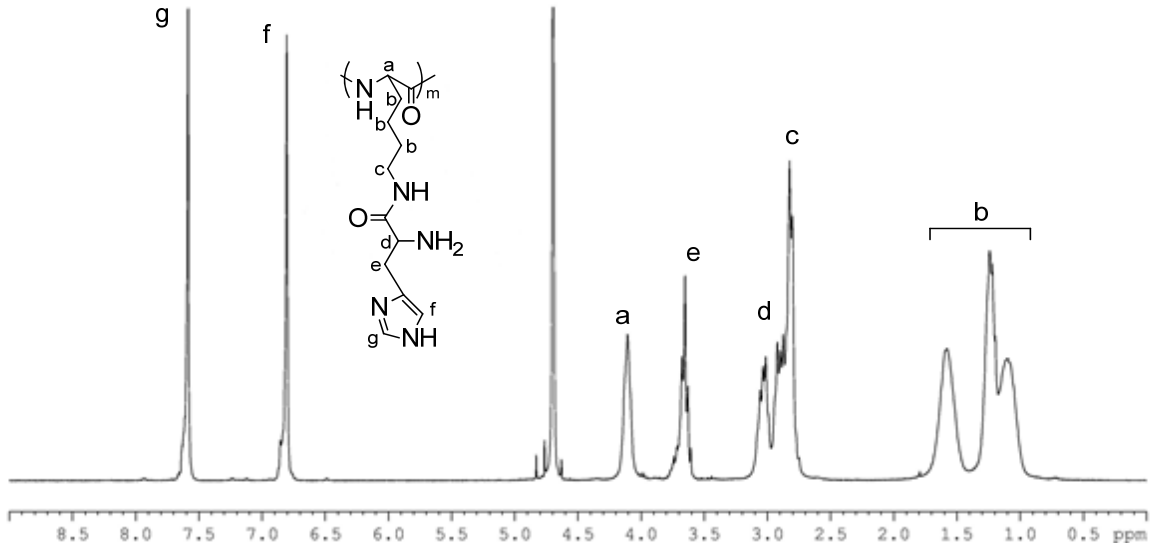

(b)

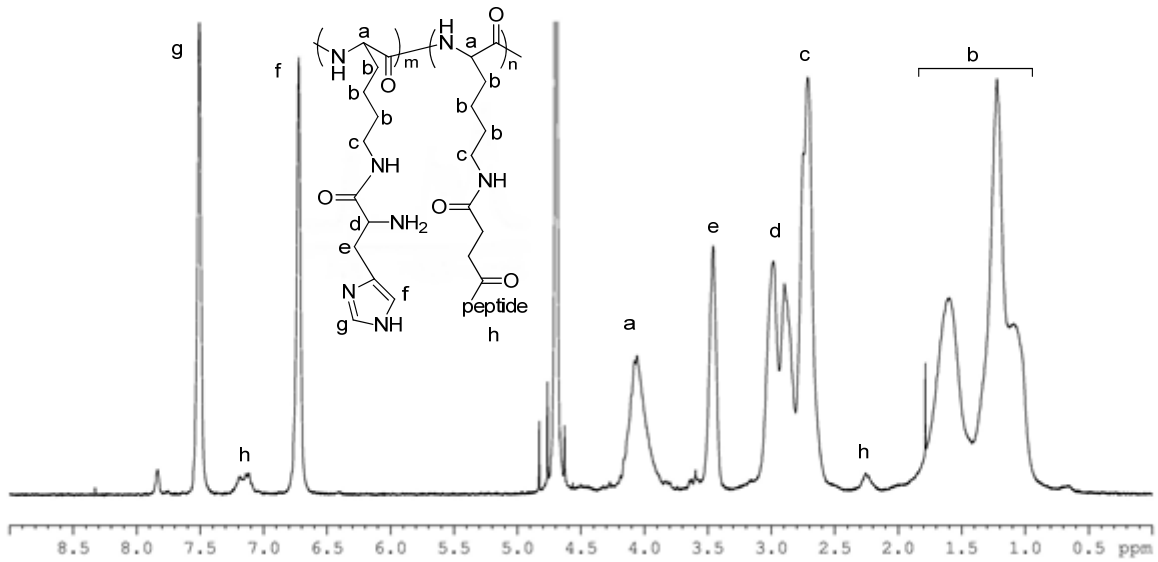

Figure 2-3. ^{1}H-NMR spectrum of (a) P-H and (b) PS-H in D_2O.

Table 2-2. Histidine and peptide content in the synthesized polymers, calculated from their NMR spectrum.

ID	Histidine content (mol%)	Peptide content (mol%)	Peptide grafting number/chain
PS-H	81	2.9	2.2
PA-H	81	3.3	2.5
PS	-	6.2	4.7
PA	-	5.0	3.8
P-H	98	-	-

2-2-2 Protonation profiles of polymers

The buffering capacity of the polymers was evaluated by acid-base titration in 150 mM aqueous NaCl solution (Figure 2-4). In the case of PLL, the pH of the solution jumped from 8 to 3 over a narrow range of added volumes of 1.0 M HCl, which means that most of the amine groups are protonated at neutral pH and exhibit weak buffering capacity in the pH range, corresponding to the acidification that occurs during maturation of the endosome (from pH 7.4 to pH 5.5). In contrast, the pH of the solution containing histidine-modified polymers (both P-H and PS-H) shows only a gradual change, from 10 to 3, over a wide range of added volumes of 1.0 M HCl. The buffering capacity results from the protonation of the α-amine and imidazole groups on the histidine residues. The buffering effect in the endosome may facilitate the endosomal escape of the polyplex formed from histidine-modified polymers due to the strong proton sponge effect.

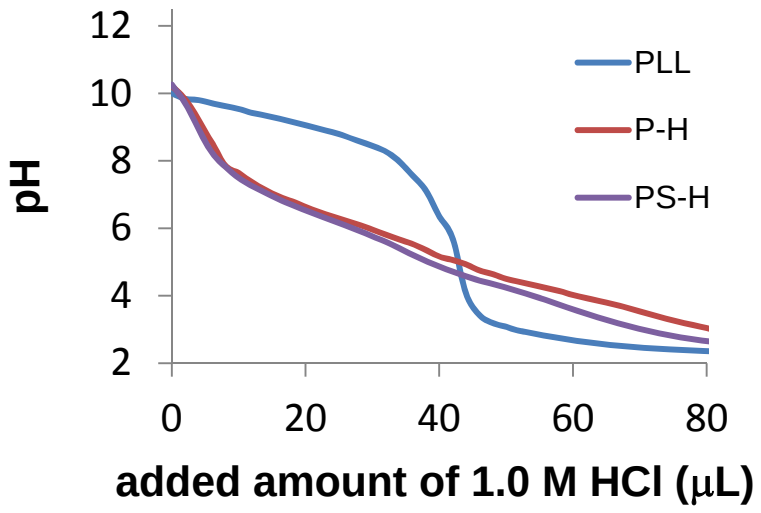

Figure 2-4. pH titration of polymers. Each polymer was dissolved in 2.0 mL of 150 mM NaCl to a final concentration of 0.1 M in monomer units. After adjusting to pH 10, the solution was titrated with 1.0 M HCl to the desired pH.

2-2-3 Ability of polymer to condense DNA at different pH

We used the ethidium bromide (EtBr) exclusion assay to examine the ability of the polymers to condense pDNA at two different values of pH. The degree of protonation at different pH was also confirmed in this way. Figure 2-5a shows the result for each polymer at pH 7.4. In this plot, each histidine residue was treated as two charges. The relative fluorescence intensity (RFI) of all four polymers decreased until an N/P ratio reached at around 2, following which the RFI leveled off. The three histidine-modified polymers have nearly the same RFI, while that of PLL is much smaller. This shows that the histidine-modified polymers condense pDNA to a lesser extent than the unmodified polymer. In contrast, at pH 6.5 (Figure 2-5 (b)), the histidine-modified polymers showed a similar condensation ability to PLL. This is consistent with the results of pH titration (Figure 2-4), which reveal that the histidine is much more protonated at pH 6.5 than at

pH 7.4.

(a)

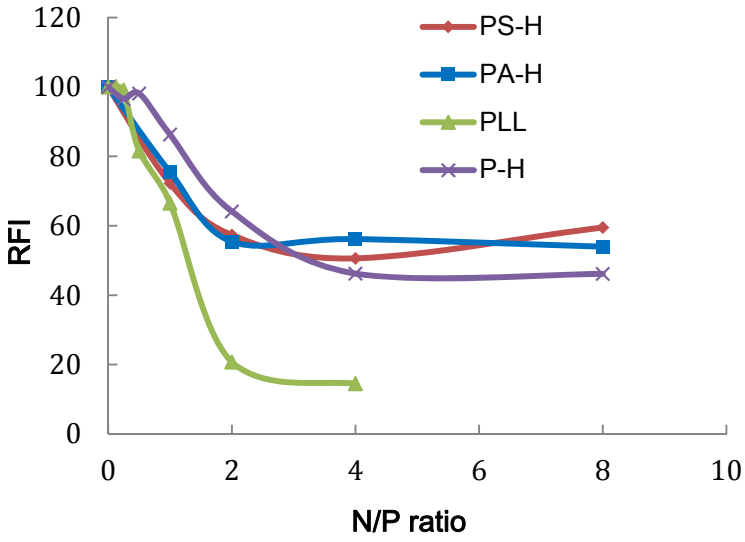

(b)

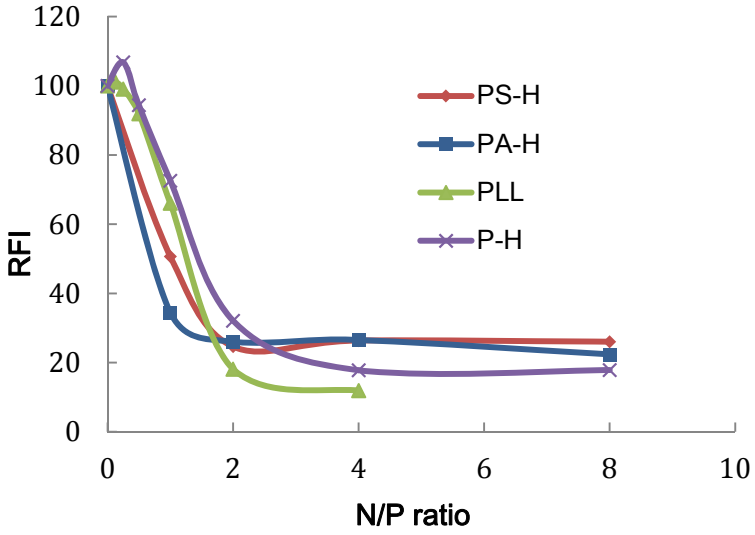

Figure 2-5: Ability of the polymers to condense pDNA at (a) pH 7.4 versus pH 6.5, and (b) in 10 mM HEPES buffer. RFI is the relative fluorescence intensity. N is the total number of amine groups in the polymers (from the peptide lysine, and the main chain lysine and histidine). Each histidine residue was treated as two charges. Data are means

± SD of three experiments.

We also measured the size and ξ-potential of the polyplex formed from these polymers at the N/P ratio of 2.5, where the condensation of pDNA is almost completed, as shown in Figure 2-5. Table 2-3 shows that the polyplexes of histidine-modified polymers (PS-H and PA-H) have a similar ξ-potential to that of unmodified polymers (PS and PA). The polyplexes prepared from histidine-modified polymers are much larger in size than the histidine-unmodified polymers, which is consistent with the weaker condensation ability of histidine-modified polymers as a result of their lower protonation degree.

Table 2-3. Diameter and ξ-potential of polyplexes in 10 mM HEPES buffer (pH = 7.4) prepared at N/P = 2.5.

ID	Diameter (nm)	ξ-potential (mV)
PS-H	234.4 ± 3.6	12.1 ± 0.7
PA-H	214.5 ±2.3	11.7 ± 0.4
PS	70.9 ± 5.3	13.7 ± 2.3
PA	71.5 ± 1.1	13.6 ± 8.4

2-2-4 Cellular uptake of polyplex

We evaluated the efficiency of cellular uptake of the polyplexes. The polyplexes were prepared from YOYO-1-labeled pDNA, and polymers at an N/P ratio of 10, in Opti-MEM (pH 7.4). As shown in Figure 2-6, the cellular uptake of the PA-H and PS-H polyplexes is almost identical. However, their cellular uptake is lower than that of PLL. This is because of the weaker condensation ability of the histidine-modified polymers,

as revealed by the ethidium bromide exclusion assay (Figure 2-5a). We then examined the cellular uptake of PS-H at a lower pH of 6.5, at which the histidine of polymer would be protonated and the polyplex should show higher condensation ability (Figure 2-5b). The cellular uptake of PS-H at pH 6.5 is even higher than that of PLL, which is consistent with the higher stability at lower pH of the polyplexes that were formed from histidine-modified polymers.

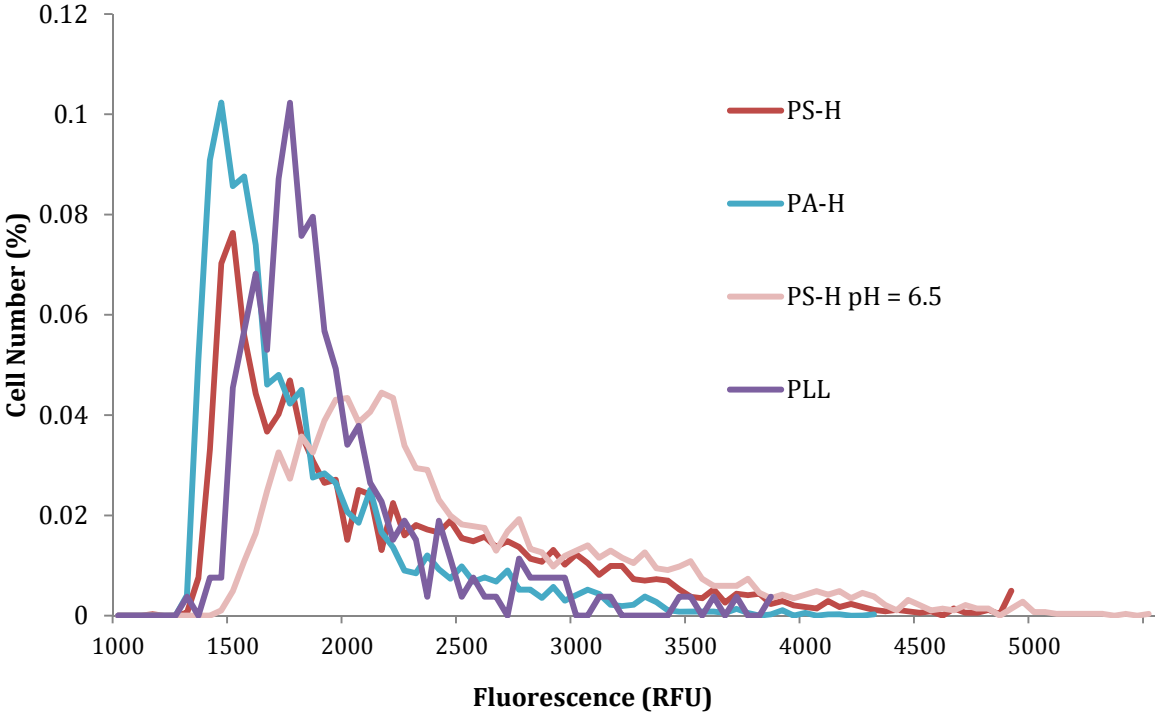

Figure 2-6. Cellular uptake of polyplex prepared at N/P = 10 in the U87-MG cell line. Cellular uptake was examined at pH 7.4 unless otherwise described. RFU means relative fluorescence units.

2-2-5 *In vitro* cytotoxicity

We examined the *in vitro* cytotoxicity of the polymers by the WST-8 assay. As

shown in Figure 2-7, the polyplexes cytotoxicity of both PLL and PEI increased with increasing N/P ratio. The cell viability dropped to 60% at N/P = 40. The high cytotoxicity of PLL and PEI results from their high charge density, which causes them to strongly interact with the cell membrane [8]. In contrast, the histidine-modified PLL (P-H) showed almost negligible toxicity even at N/P = 40, which is a result of its lower charge density owing to the lower pK_a of imidazole and the α-amine group of histidine residue as revealed by pH titration (Figure 2-4).

As for the peptide-modified polymers, a similar effect of the histidine residue was observed, where the histidine-modified polymers (PS-H and PS-A) exhibited lower toxicity than the unmodified polymers (PS and PA). The lower cytotoxicity of PS-H and PS-A may contribute to increasing the gene expression in transfected cells.

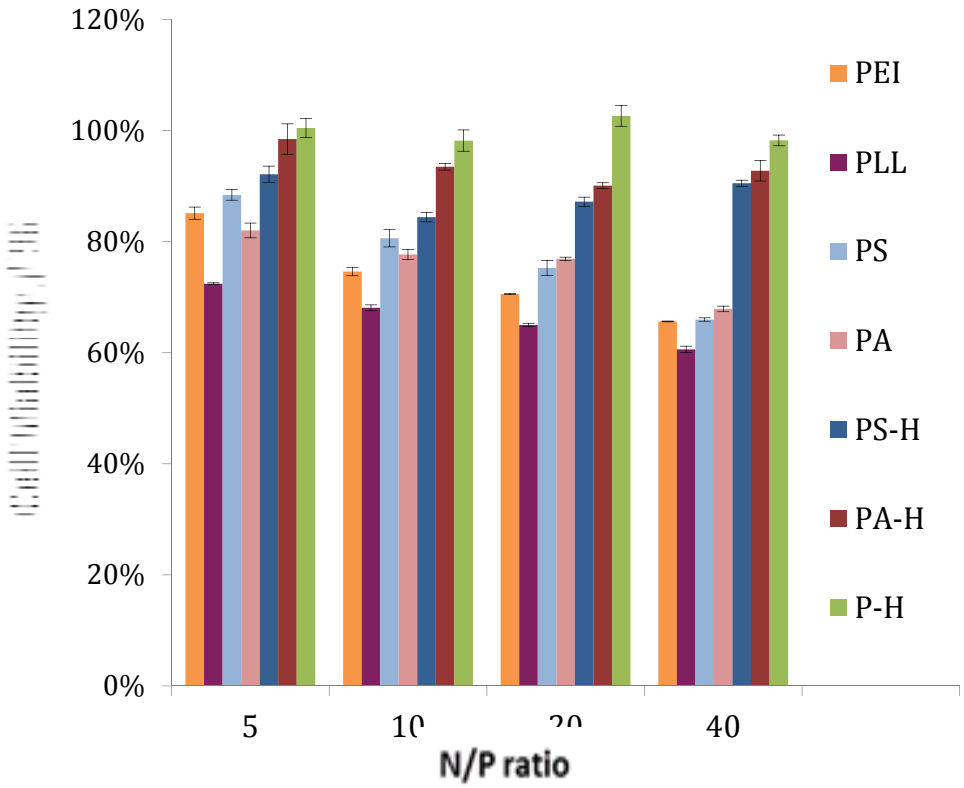

Figure 2-7. Cytotoxicity of polymers against the U87-MG cell line, investigated by the WST-8 assay. Polyplexes of each polymer were prepared at different N/P ratios and incubated with U87-MG cells in Opti-MEM at 37 °C for 4 h. The cell viability was standardized by non-treated cells. Data are means ± SD of three experiments.

2-2-6 *In vitro* transfection

We examined the PKCα-responsive gene expression of these polymers by using U87-MG and B16 melanoma cell lines, in both of which the PKCα is hyper-activated [34, 35]. Figure 2-8a shows the results for the U87-MG cell line. At higher N/P ratios (from 10 to 60), the PKCα-responsive gene expression with PS-H carrier was higher than that with PA-H (the negative control). This result clearly indicated that a suppression of gene expression in the negative control PA-H and the PKCα-responsive gene expression in PS-H. The difference in the gene expression between PS-H and PA-H was about ten-fold at the N/P ratios of 10 and 40. Similar results were obtained for the B16 melanoma cell line (Figure 2-8b), in which the PKCα activity is nearly equal to that in U87-MG cell line [3, 26].

As for the effect of histidine modification, PS-H showed 5- to 10-fold higher gene expression than PS at the N/P ratios of 10, 40, and 60 (Figure 2-8a). The enhanced ability of PS-H to promote gene expression results from the buffering effect of the histidine residues.

The histidine-unmodified polymers also showed PKCα-responsive gene expression (Figure 2-8 a and b). However the PKCα-responsive gene expression was only observed over a narrow range (N/P = 10) and the difference between PA and PS was small. These results show that histidine modification of the polymer can widen the applicable range

of N/P ratios, and increase the differences in the gene expression observed for PKCα-responsive versus non-responsive carriers.

(a)

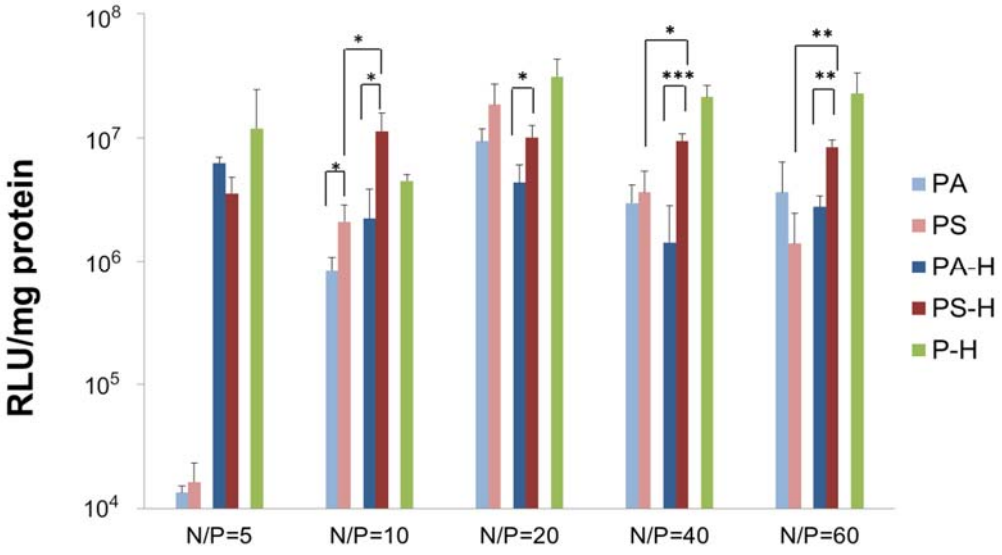

(b)

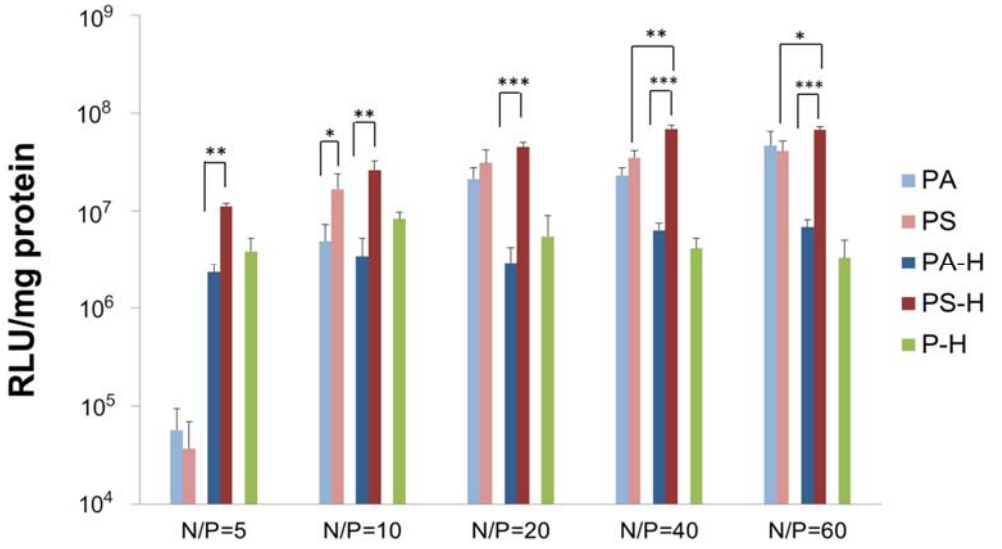

Figure 2-8. *In vitro* transfection efficiency of (a) U87-MG and (b) B16 melanoma cell

lines, measured via luciferase assay. ***$P < 0.001$, **$P < 0.01$, and *$P < 0.05$. Data are means ± SD of three experiments.

2-2-7 Time-dependent gene expression

The time-dependent profile of the luciferase gene expression in U87-MG cells was monitored by AB-2500 Kronos Dio, which allows continuous measurement of luciferase expression from the living cells. After 4 h from the transfection with each polyplex, the cells were cultured with fresh medium containing 200 μM D-luciferin, and the bioluminescence from the expressed luciferase was monitored at 20-min intervals [36]. As shown in Figure 2-9, the gene expression from the complex with PS-H was observed 4 h from the start of the transfection, and continued for more than 20 h, exhibiting a slight increase over this time period. In contrast, PA-H showed almost negligible gene expression in the first 10 h. PKCα-responsive gene expression, and the endosomal escape of the PS-H polyplex, occurred immediately upon the cellular uptake of the polyplex, that is, within 4 h from the start of the transfection. The P-H polyplex showed much higher gene expression than PLL, which may be because of the relative ease with which it escapes the endosome, although the cellular uptake of P-H is lower than that of PLL (data not shown). Notably, the gene expression of PA-H is more suppressed than that of P-H, indicating that the cationic peptides on the histidinylated PLL prevent the dissociation of the polyplex.

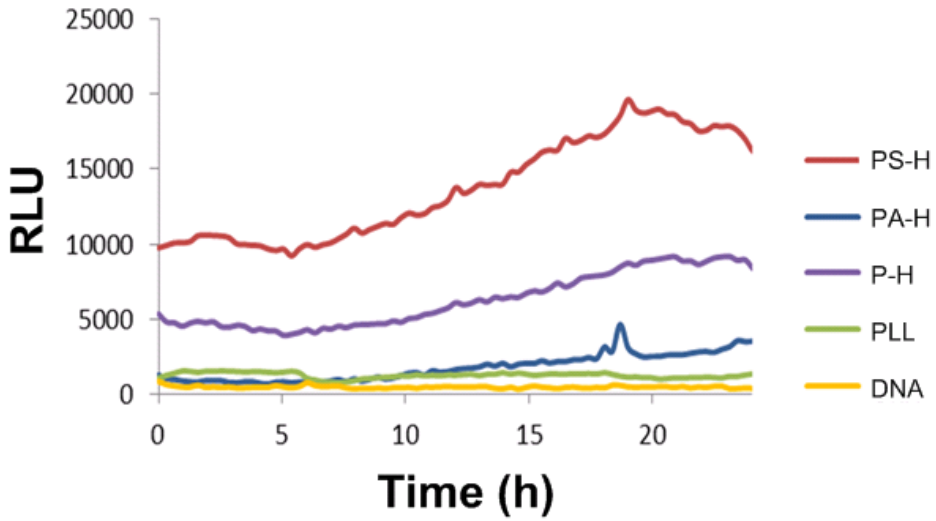

Figure 2-9. Time-dependent gene expression of the U87-MG cell line from each polyplex formed at N/P = 10. The cells were transfected with each polyplex in Opti-MEM for 4 h, followed by incubation in MEM containing 10% FBS and 200 μM D-luciferin. The time shown on the x-axis begins at t = 0 corresponding to 4 h after the transfection.

2-2-8 Intracellular distribution of polyplexes

To gain insight into the influence of histidine modification on the endosomal escape of the polyplex, the intracellular distribution of the various polyplexes (N/P = 10) in Huh-7 cells was monitored by con-focal laser scanning microscope after 24 h of transfection. The pDNA was labeled with Cy5 and the endosome/lysosome system was stained with LysoTracker Green. As shown in Figure 2-10, the polyplex of PS-H clearly achieved endosomal escape of the Cy5-labeled pDNA, shown as red dots (colocalization coefficient = 0.63 ± 0.07). This result was similar to that of LPEI, whose colocalization coefficient was 0.57 ± 0.11. In contrast, the low endosomal escape ability

of PS and PLL was confirmed by the presence of the yellow dots resulting from the colocalization of Cy5-labeled pDNA in endosomes and lysosomes. The colocalization coefficients of PS and PLL were 0.81 ± 0.05 and 0.83 ± 0.07, respectively. The difference between the histidine-modified polymer (PS-H) and the non-modified polymer (PS) was significant ($p < 0.005$). Thus, the endosomal escaping ability of the polyplex formed from the PS-H should reflect its more effective buffering capacity.

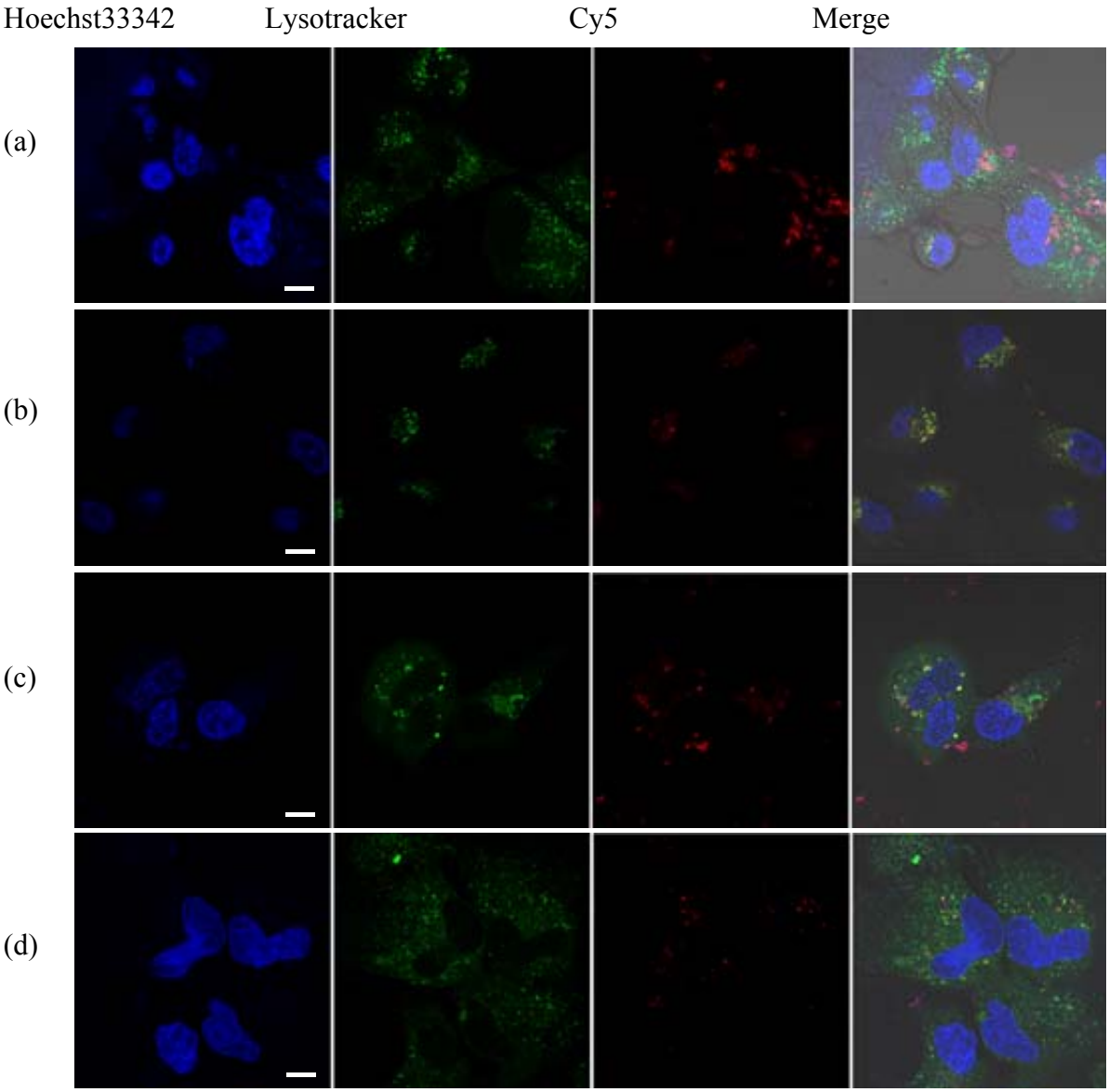

Figure 2-10. Intracellular distribution of pDNA that was taken up as part of polyplexes

prepared at N/P = 10 from (a) PS-H, (b) LPEI, (c) PS, and (d) PLL. The CLSM observation was performed at 24 h after transfection. pDNA was labeled with Cy5 (red). Late endosomes/lysosomes and the nuclei were stained with LysoTracker Green (green) and Hoechst 33342 (blue), respectively. The scale bar represents 20 μm.

2-3 Conclusion

We designed cancer-specific gene carriers by modifying PLL with histidine to improve the buffering capacity, and with cationic substrate peptides to improve the cancer specific gene expression. These polymeric carriers were synthesized easily by functionalizing the PLL main chain with the protected peptide and histidine, followed by deprotection of the functional groups. These polymers could condense pDNA to polyplexes of an appropriate size for cellular uptake. The buffering capacity of the histidine allowed the polyplexes to effectively escape from the endosome. The carriers showed a clear improvement in the PKCα-responsive expression of pDNA in cancer cells. Therefore, our PLL-based gene carriers are a new class of protein-kinase-responsive gene carriers, potentially applicable to any protein kinases that are activated specifically in cancer cells.

2-4 Experiment Methods

Preparing of the pCMV-luc2 DNA

To preparing the luciferase encoding pDNA, the luciferase gene fragment was extract from the luciferase encoding cDNA, and inserted into pcDNA3. The recombined pCMV-luc2 was amplified in E. coli and purified by QIA fileter

Synthesis of PKCα–specific substrate peptide

The protecded peptides were synthesized by the solid-phase method using the Sieber Amide resin (Merck, Hohenbrunn, Germany) (0.69 mmol/g). In the condensation reaction, the n-terminal protected amino acid (4 eq.)、HOBt·H_2O (4 eq.) 、HBTU (4 eq.) 、DIPEA (8 eq.) was mixed in DMF, and reacted at r.t. for 10 min. The end of each reaction was confirmed by Kaiser Test. After the condensation of the last amino acid, the N-terminus of the peptide was reacted with succinic anhydride in 0.9 M DIPEA/NMP. The peptide was then cleaved from the resin with the remaining protective groups by treating with 1% TFA in DCM solution, and the resulting solution was neutralized by 10% pyridine in methanol. The obtained protected peptide was reprecipitated using cold water and then dried in vacuo. The target peptide was confirmed by MALDI-TOF-MS (Bruker JapanCo., ltd., Tokyo, Japan) without deprotection. The purity of the protected peptides was determined by high-performance liquid chromatography (HPLC).

Synthesis of polymer

The synthesis of the carriers was conducted following Scheme 1. PLL·HBr was

dialyzed against a solution of 0.1% TFA in water and lyophilized. The resulting PLL·TFA (27 mg; 0.11 mmol of ε–NH_2) was dissolved in 500 μL DMF. Then, the protected peptide (15 mg; 6.4 μmol) dissolved in 2.5 mL DMF was added to the PLL·TFA solution, following which HBTU (2.5 mg; 6.4 μmol) and HOBt (0.9 mg; 6.4 μmol) were added as coupling reagents. To this solution, 80 μL of DIEPA was added to adjust the pH from 9 to 10. After reacting for 2 days, Fmoc-His (Trt)-OH (206 mg; 0.33 mmol), HBTU (126 mg; 0.33 mmol), and HOBt (45 mg; 0.33 mmol) were added to further modify the rest of the amine groups on the PLL. After reacting for 4 h, the completion of the reaction was confirmed by the Kaiser test.

The resulting polymer was reprecipitated in cold acetyl acetate, and then the Fmoc group was deprotected by adding 20% PPD in DMF. After 10 min, the polymer was precipitated again in cold acetyl acetate. The remainder of the protecting groups were removed by dissolving the polymer in a mixture of 95% trifluoroacetic acid, 2.5% triisopropylsilane, and 2.5% water. After 2 h, the polymer was purified by reprecipitation with cold acetyl acetate three times. The obtained white powder was dissolved and dialyzed against distilled water for 3 days in a semi-permeable membrane bag with a molecular weight cutoff of 3,000 Da. After lyophilization, the final product was obtained as a white powder. The content of the peptide and histidine in the polymer was estimated by ^{1}H NMR spectrum in D_2O using a 300 MHz spectrometer.

Polyplex formation

To prepare polyplexes at various N/P ratios (the ratios of moles of the amine groups and imidazole groups of polymers to those of the phosphate ones of pDNA), 25 μL of 0.1 mg/mL pDNA (pCMV-luc2) and 25 μL polymer solution were diluted by adding

475 μL of 10 mM HEPES (pH 7.4), following which the resulting solutions were mixed and then incubated at room temperature for 30 min. The polyplex diameter and ζ-potential were measured by a Zetasizer (Malvern Instruments, Worcestershire, UK) with a He/Ne laser at a detection angle of 173° at 25 °C.

Ability of polymers to condense DNA at different pH

To check the ability of the polymers to condense DNA, 5 μL of 0.1 mg/mL plasmid DNA was mixed with 1.5 μL of 0.1 mg/mL EtBr. After incubating this mixture for 10 min, 5 μL polymer solution at each N/P ratio was added and the total volume of solution was diluted to 100 μL by adding 10 mM HEPES. After 30 min, its fluorescence intensity was measured by multi-label counter ARVO (Wallac Incorporated, Turku, Finland) (λ_{ex} = 530 nm, λ_{em} = 590 nm, 20 s). The relative fluorescence intensity (RFI) was determined using the following equation: RFI = $(F_{sample}-F_e)/(F_0-F_e)$, where F_{sample}, F_e, and F_0 are the fluorescence intensities of the polyplex, background, and free pDNA without carrier, respectively.

pH titration

Each polymer (0.1 M in repeating unit of backbone polymer) was dissolved in 2.0 mL of 150 mM NaCl. After adjusting to pH 10 with 1.0 M NaOH, the solution was titrated with 80 μL of 1.0 M HCl to the desired pH, which was monitored by AUT-701 (TOA-DKK, Japan).

Cell culture

B16 cells, HepG2 cells and Huh-7 cells were cultured in D-MEM containing 10%

fetal bovine serum (FBS), 100 U/mL penicillin, 100 μg/mL streptomycin and 0.25 μg/mL amphotericin B (all from Gibco Life Technologies, Grand Island, NY, USA) under a humidified atmosphere containing 5% CO_2 and 95% air at 37 °C. U87MG cells were cultured in MEM containing the same supplements under 5% CO_2 and 95% air at 37 °C.

Cytotoxicity assay

Cytotoxicity of the polymers was evaluated by measuring cell viability. U87MG cells were plated in a 96-well plate at an initial density of 10,000 cells per well in 500 μL of MEM containing 10% FBS for 24 h. Polyplexes (polycation/pDNA complexes) were prepared by mixing pDNA (1 μg) with the polymer at each N/P ratio, and incubating this mixture for 30 min at room temperature. Just before transfection, the culture medium was exchanged for Opti-MEM (GIBCOy BRL) without serum. Polyplex solutions were then added, and samples were incubated for 4 h at 37 °C, 5% CO_2, following which the Opti-MEM was exchanged for growth medium. The metabolic activity of the cells was measured 24 h later by WST-8 assay. Briefly, 10 μL of CCK-8 and 90 μL of MEM containing 10% FBS was added to the cell. After culturing for 1 h, the absorption was measured by multilabel counter ARVO at 450 nm.

Transfection study

pDNA coding luciferase (pCMV-Luc2) was used for transfection. U87MG and B16 cells were respectively plated in MEM or DMEM containing 10% FBS, at a density of 2×10^4 cells/well in a 48-well plate, and then incubated for 24 h. Polyplexes were prepared by mixing pDNA (1 μg) with a polymer at each N/P ratio and incubating for

30 min at room temperature. Just before the transfection procedure, the culturing medium was exchanged for Opti-MEM without serum. Polyplex solution was added, and the cells were incubated for 4 h at 37 °C, 5% CO_2. The solution of polyplex and Opti-MEM was then replaced with 500 μL of fresh culturing medium containing 10% FBS, and the cells were further incubated at 37 °C, 5% CO_2 for 24 h. The cells were washed with PBS and lysed for 20 min with 100 μL of lysis buffer (20 mM Tris-HCl containing 0.05% TritonX-100 and 2 mM EDTA (pH 7.5)). The 10 μL of lysate were mixed with 40 μL of luciferase assay solution (Promega), following which the luminescence of the mixture was measured with a luminometer.

Cellular uptake of polyplex

To prepare YOYO-1 labeled pDNA (pCMV-Luc2), 500 μ of 0.1 μg/ μL pDNA was mixed with 100 μL of 10x TAE buffer and 400 μL of 10 μM YOYO-1 containing TE buffer. The solution was mixed for at least 1 h at room temperature in the dark, and then stored at −20 °C. To prepare the polyplex, the N/P ratio of each polymer mixture, containing 1 μg pDNA was first adjusted to 10, in 10 mM HEPES buffer at pH 6.5 or 7.4. The mixture was then incubated for 15 min. Before transfection, 40 μL of this solution was mixed with 460 μL of pH-adjusted Opti-MEM. The U87MG cell line was seeded on a 24-well plate (50,000 cells/well), in MEM containing 10% FBS, and incubated at 37 °C for 24 h. After washing the cells with PBS, the polyplex solution was added into each well and incubated for 2 h The cells were washed again with PBS, harvested with Trypsin-EDTA (Gibco), and analyzed using a Tali image-based cytometer (Invitrogen).

Time-dependent monitoring of in vitro transfection

HepG2 cells and U87MG cells were seeded in 35-mm plastic culture dishes and incubated for 24 h in 2 mL of DMEM or MEM containing 10% FBS before transfection. The cells were then incubated with the polyplex (4 μg of pCMV-Luc2/dish) at N/P = 10 in 2 mL Opti-MEM. After culturing for 4 h, the medium was exchanged with fresh medium containing 200 μM D-luciferin and 10 mM HEPES. The dishes were then set in a luminometer (AB-2500 Kronos Dio, ATTO Co., Tokyo, Japan), and their bioluminescence was monitored every 20 min (1-min collection time) in DMEM containing 10% FBS.

Confocal laser scanning microscope (CLSM) bbservation

pDNA (pCMV-Luc2) was labeled with Cy5 using the Label IT Nucleic Acid Labeling Kit (Mirus, Madison, WI, USA) according to the manufacturer's protocol. Huh-7 cells were seeded at a density of 1×10^5 cells in 35-mm non-coated glass bottom culture dishes and incubated for 24 h in 2 mL of MEM containing 10% FBS before transfection. LPEI (25kDa) and PLL (Mw 15,000–30,000) were used as the positive and negative controls, respectively. Polyplexes were prepared by mixing the Cy5-labeled pDNA (2 μg) with the polymer at N/P = 10 and incubating the mixture for 30 min at room temperature. Just before the transfection procedure, the culturing medium was exchanged for 1 mL Opti-MEM without serum. Polyplex solution was added, and the cells were incubated for 4 h at 37 °C, 5% CO_2. The polyplex and Opti-MEM solution were then removed and cells were further incubated for 24 h at 37 °C, 5% CO_2 in 2 mL of fresh culturing medium containing 10% FBS. Fifteen minutes prior to imaging the cells, the acidic late endosomes and lysosomes were stained with LysoTracker Green

and the nuclei were stained with Hoechst 33342 (Molecular Probes, Eugene, OR, USA). Polyplexes were observed by CLSM (ZEISS LSM 700; Carl Zeiss, Oberlochen, Germany) with a Plan-Apochromat 63×/1.40 Oil Ph3 M27 objective. The colocalization coefficient, which measures the fraction of red Cy5-labeled DNA pixels that also indicate a positive signal for LysoTracker-green, was obtained using the Zeiss LSM 2011 imaging software ($n > 10$) with a calculation of $pixels_{colored}/pixels_{totalred}$. $Pixels_{colored}$ refers to the colocalized red pixels while $pixels_{totalred}$ refers to the total red pixels. A colocalization of 1 means complete colocalization, whereas 0 means no colocalization.

2-5 Refenrence

[1] Kenji Kawamura, Jun Oishi, Jeong-Hun Kang, Kota Kodama, Tatsuhiko Sonoda,Masaharu Murata, Takuro Niidome, and Yoshiki Katayama *Biomacromolecules* **2005**, 6, 908-913

[2] Riki Toita , Jeong-Hun Kang, Jong-Hwan Kim, Tetsuro Tomiyama, Takeshi Mori,Takuro Niidome, Byungdug Jun, Yoshiki Katayama *J. Control. Release* **2009**,139, 133–139

[3] Tetsuro Tomiyama, Jeong-Hun Kang, Riki Toita, Takuro Niidome and Yoshiki Katayama, *Cancer Sci.*, **2009**, 100, 1532-1536

[4] Tetsuro Tomiyama, Riki Toita , Jeong-Hun Kang, Daisuke Asai, Shujiro Shiosaki, Takeshi Mori,Takuro Niidome, Yoshiki Katayama, *J. Control Release* **2010**, 148, 101-105

[5] Akira Tsuchiya, Yuki Naritomi, Satoshi Kushio, Jeong-Hun Kang, Masaharu Murata, Makoto Hashizume, Takeshi Mori, Takuro Niidome, Yoshiki Katayama, *J. Biomed. Mater Res.* **2012**, 100A, 1136-1141

[6] Riki Toita, Jeong-Hun Kang, Tetsuro Tomiyama, Chan Woo Kim, Shujiro Shiosaki, Takuro Niidome, Takeshi Mori, and Yoshiki Katayama, *J. Am. Chem. Soc*. **2012**, 134, 15410−15417

[7] Chan Woo Kim, Riki Toita, Jeong-Hun Kang, Kai Li, Eun Kyung Lee, Guo Xi Zhao, Daiki Funamoto, Takanobu Nobori,, Yuta Nakamura, Takeshi Mori, Takuro Niidome, Yoshiki Katayama, *J. Control Release* **2013**, 170, 469-476

[8] Dagmar Fischer, Youxin Li, Barbara Ahlemeyer, Josef Krieglstein, Thomas Kissel, *Biomaterials* **2003**, 24,1121-1131

[9] Jong Eun Ihm, Ki-Ok Han, Chang Sun Hwang, Jong Hee Kang, Kwang-Duk Ahn,

In-Kwon Han, Dong Keun Han, Jeffrey A. Hubbell, Chong-Su Cho *Acta Biomaterialia*, **2005**, 1, 165–172.

[10] David Putnam, Christine A. Gentry, Daniel W. Pack, and Robert Langer *Proc. Nat.l Acad. Sci. USA* **2001**, 98, 1200-1205

[11] Harry Mellor and Peter J. Parker, *Biochem. J.* **1998**, 332, 281-292

[12] J Moscat, MT Diaz-Meco and MW Wooten, C*ell Death and Differentiation*, **2009**, 16, 1426–1437

[13] Riner, E.M., Kazanietz, M.G., *Nat. Rev. Cancer*, **2007**, 7, 281

[14] Steinberg, S.F., *Physiol. Rev.*, **2008**, 88, 1341

[15] Daria Mochly-Rosen, Kanad Das and Kevin V. Grimes, *Nat. Rev. Drug Discovery*, **2012**, 11, 937-957

[16] P. Cohen, *Eur. J. Biochem.*, **2001**. 268, 5001-5010

[17] J. R. Gruber, S. Ohno, R. M. Niles, *J. Biol. Chem.*, **1992**, 267, 13356-13360

[18] M. Oka, U. Kikkawa, *Cancer and Metastasis Rev.*, **2005**, 24, 287-300

[19] D. T. Yamanishi, F. L. Meyskens Jr., *Crit. Rev. Oncogen.*, **1994**, 5, 429-450

[20] E. Batlle, J. Verdu, D. Dominguez, M. M. Llosas, V. Diaz, N. Loukili, R. Paciucci, F. Alameda, A. G. de Herreros, *J. Biol. Chem.*, **1998**, 273, 15091-15098

[21] P. Cornford, J. Evans, A. Dodson, K. Parsons, A. Woolfenden, J. Neoptolemos, C. S. Foster, *Am. J. Pathol.*, **1999**, 154, 137-144

[22] C. A. O'Brian, V. G. Vogel, S. E. Singletary, N. E. Ward, *Cancer Res.*, **1989**, 49, 3215-3217

[23] W. Zwart, A. Griekspoor, V. Berno, K. Lakeman, K. Jalink, M. Mancini, J. Neefjes, R. Michalides, *EMBO J.*, **2007**, 26, 3534-3544

[24] C. A. M. La Porta, L. Tessitore, R. Comolli, *Carcinogenesis*, **1997**, 18, 715-719

[25] C. A. M. La Porta, R. Comolli, *Carcinogenesis*, **1994**, 15, 1743-1747

[26] Kang, J.-H., Asai, D., Yamada, S., Toita, R., Oishi, J., Mori, T., Niidome, T., Katayama, Y. Proteomics 2008, 8, 2006–2011.

[27] Wang, D. A., Narang, A. S., Kotb, M., Gaber, A. O., Miller, D. D., Kim, S. W., Mahato, R. I. *Biomacromolecules* **2002**, 3, 1197-1207.

[28] Aravindan L, Bicknell KA, Brooks G, Khutoryanskiy VV, Williams AC., *Int J Pharm*. **2009,** 13,201-210

[29] Neu, M., Fischer, D., Kissel, T. *J. Gene Med.* **2005**, *7*, 992–1009.

[30] Kanjiro Miyata, Makoto Oba, Masataka Nakanishi, Shigeto Fukushima, Yuichi Yamasaki, Hiroyuki Koyama, Nobuhiro Nishiyama, and Kazunori Kataoka, *J. Am. Chem. Soc*. **2008**, *130*, 16287–16294

[31] Patrick Midoux and Michel Monsigny *Bioconjugate Chem.* **1999**, *10,* 406-411

[32] Christine Gonc¸alves, Chantal Pichon, Brigitte Gue´rin, Patrick Midoux*, J. Gene Med.* **2002**, 4, 271–281

[33] Takuya Wada, Arihiro Kano, Naohiko Shimada, and Atsushi Maruyama, *Macromolecular Research* **2012**, 20, 302-308

[34] Jeong-Hun Kang, Daisuke Asai, Jong-Hwan Kim, Takeshi Mori, Riki Toita,Tetsuro Tomiyama, Yoji Asami, Jun Oishi, Yuko T. Sato, Takuro Niidome, Byungdug Jun,Hideki Nakashima, and Yoshiki Katayama *J. Am. Chem. Soc.* **2008**, 130, 14906–14907

[35] Riki Toita, Jeong-Hun Kang, Tetsuro Tomiyama, Chan Woo Kim, Shujiro Shiosaki, Takuro Niidome, Takeshi Mori, and Yoshiki Katayama *J. Am. Chem. Soc.* **2012**, 134, 15410−15417

[36] Seiji Takae, Kanjiro Miyata, Makoto Oba, Takehiko Ishii, Nobuhiro Nishiyama,

Keiji Itaka, Yuichi Yamasaki, Hiroyuki Koyama and Kazunori Kataoka, *J. Am. Chem. Soc.* **2008**, 130, 6001-6009

Chapter 3 Akt-responding system with higher gene expression efficiency

3-1 Introduction

In the chapter 2, we designed cancer-specific gene carriers by modifying PLL with histidine to improve the buffering capacity, and with cationic substrate peptides to improve the cancer specific gene expression. The peptide group is designed to work as phosphorylation motif and cationic charge motif. The histidine group is to work as buffering motif and to reduce the cytotoxicity of PLL main chain. This polymer showed good buffering capacity, and about 10 times difference of gene expression level between this polymer and its control. But the transfection efficiency did not come up to our expectations. Though the grafted peptide motif was designed as the cationic center, ability of the DNA condensation and the cellular uptake seems quite low. This may limit the transfection efficiency of this polymer as gene carrier. To further improve this polymer, we tried to optimize the modification ratio of histidine. And to widen its scope, in this chapter we focused on Akt1, another hyper-activated protein kinase in many kinds of cancer cells.

3-2 Protein kinase B (PKB, or Akt)

Akt (also known as PKB) was first identified by Stephen Staal in 1987 as the likely transforming gene component, v-Akt, of the Akt8 provirus[1]. The kinase domain of Akt is similar to that of protein kinase A (PKA) and protein kinase C (PKC), therefore it was termed Related to A and C[2]. Akt is a serine/threonine protein kinase that plays a key role in multiple cellular processes such as glucose metabolism, cell proliferation, apoptosis,

transcription and cell migration.

Akt superfamily comprises three isoforms (Akt1 or PKBα, Akt2 or PKBβ, Akt3 or PKBγ). The structure of these three isoforms is highly conserved: an N-terminal pleckstrin homology (PH) domain, a kinase catalytic domain and a C-terminal regulatory tail containing a hydrophobic motif [3-5] (Fig. 3-1). There are also two C-terminal splice variants have been reported: PKBβ1 contains a 40-amino acid C-terminal extension[6], while PKBγ1 has a unique C-terminus[7]

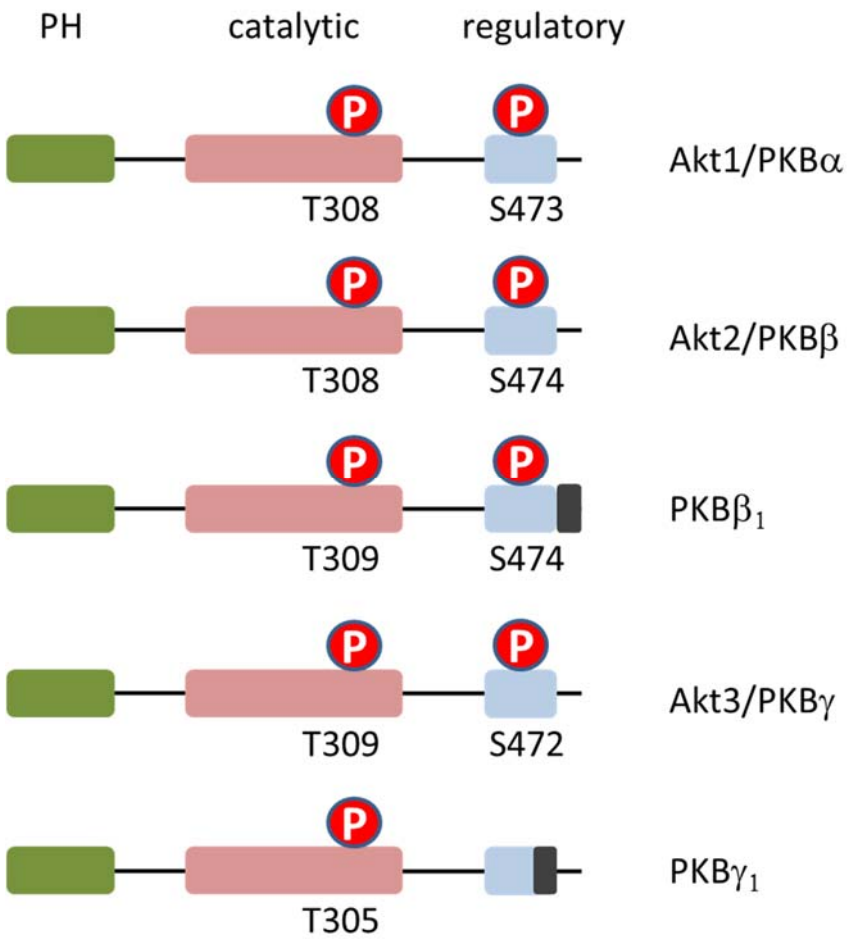

Figure 3-1: Domain structure of Akt isoforms and variants. The activating phosphorylation sites in the catalytic loop and the hydrophobic tail are indicated.

Akt is a downstream target of Phosphatidylinositide 3-kinase (PI3K), a family of related intracellular signal transducer enzymes which is comprised of 85 kDa and 110 kDa subunit. Activation of PKBα involves a PI3K and PH domain-dependent membrane translocation step, followed by phosphorylation of two key regulatory sites, Thr308 in the kinase domain and Ser473 in the regulatory domain[8, 9] (Fig. 3-2). Receptor tyrosine kinases (RTKs) are activated by the binding of growth factors (GFs) to the extracellular domain. After that, PI3K bind either directly or through an adaptor protein to the activated RTKs. PI3K then phosphorylates phosphatidylinositol-4,5-bisphosphate (PIP2) to phosphatidylinositol-3,4,5-bisphosphate (PIP3), while PTEN (phosphatase and tensin homolog deleted on chromosome ten, a phosphatase and tensin homology) reverse this reaction. The activation of Akt in this pathway can be blocked by the PI3-kinase inhibitors such as wortmannin or LY294002. Akt is normally maintained in an inactive state through an intramolecular interaction between the PH and kinase domains. In the activation process, PKB binds to PIP3 via its PH domain, where it is phosphorylated on two key residues by upstream kinases. 1, 3-phosphoinositide-dependent kinase-1 (PDK1) can access the activation loop of Akt and phosphorylate it on Thr308. Dephosphorylation of this site is regulated by protein phosphatase 2A (PP2A). Mammalian target of rapamycin (mTOR) phosphorylates Akt in the regulatory domain on Ser473 in a PI3 kinase dependent manner. Dephosphorylation of Ser473 is regulated by the phosphatase PHLPP. After being activated, Akt dissociates from the membrane and translocates to the cytosol to phosphorylate a wide range of substrates.

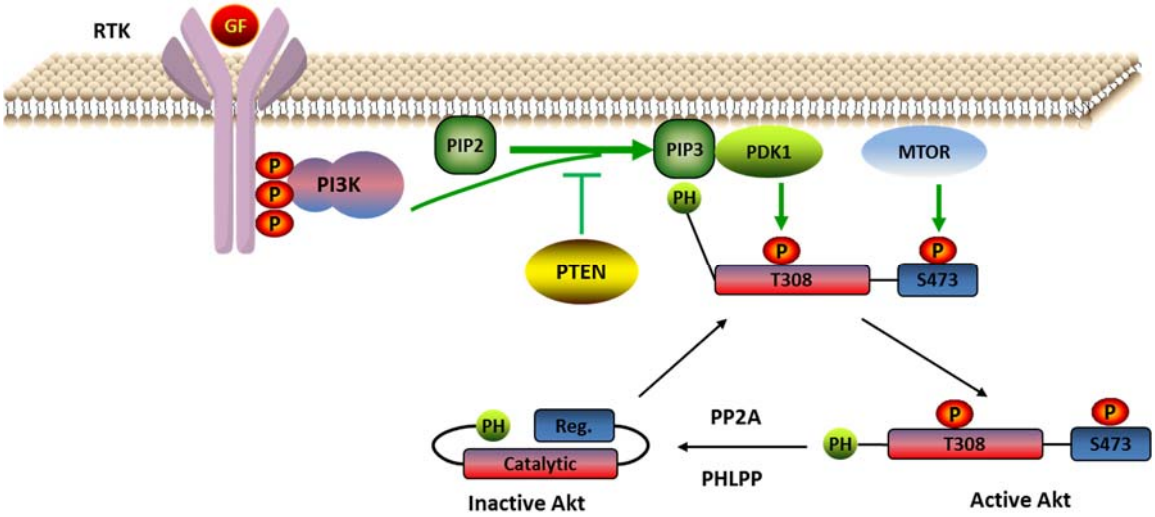

Figure 3-2: Activation and regulation of Akt.

The PI3K-Akt pathway is a main regulator of cell proliferation and survival. Hyper-activation of this pathway has been reported in many human cances, including cancers of the colon, breast, brain, liver, stomach and lung[10]. The Akt inhibitors were proved to be highly effective with a low IC_{50}, but later, they were shown to have toxic side effects and poor pharmacological properties and selectivity. Thus, these inhibitors were only effective in preclinical models (Fig.3-3)[9, 13]. 2-(4-morpholinyl)-8-phenyl-chromone (LY294002) is a specific PI3K inhibitor that acts as ATP competitive manner with an IC_{50} = 1.4 μM but not PI4K, EGFR, PDGFR, MAPK, PKA, or PKCα[26-27]. It effectively induced apoptosis in pancreatic cancer cell lines under nutrient starvation conditions[11] and greatly potentiated chemotherapy-induced apoptosis in lung cancer cells with high levels of Akt activity[12]. LY294002 is widely used in Akt research, thus this experiment also use this one as an indirect Akt inhibitor.

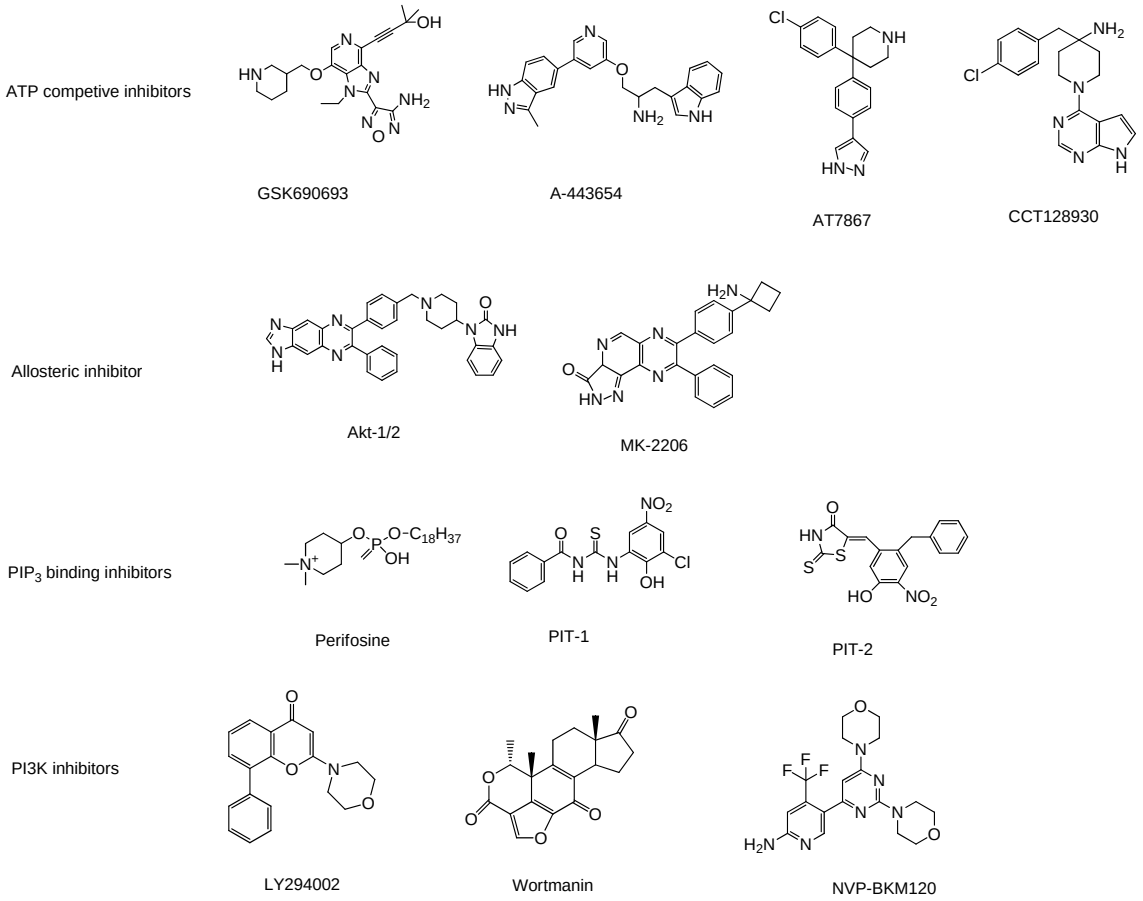

Figure 3-3: small molecule inhibitors of Akt[9, 13].

3-3 Results and discussion

3-3-1 Selection of Akt substrate

As we have described before, a specific responding substrate is critical for intracellular signaling responding gene expression. To design a Akt responding gene carrier, an Akt specific substrate is necessary. It has been identified that a minimal motif, R-X-R-X-X-S/T-, is necessary for the Akt substrate[15]. But this sequence is similar to some of the PKC substrate members[14]. To find an optimal Akt substrate, we chose 3 kinds of peptide substrates (Tab. 3-1) from the reported candidates[15-18], including three

widely applied peptides: Crosstide、Aktide and Aktide-2T. The sequence and reported Km and Vmax of the synthesized peptides are shown in Tab. 2-1

Table 3-1. Sequence、Km and V_{max} of the Akt substrates [15, 18]

Peptide sequence	K_m (μM)	V_{max} (pmol/mg/min)	V_{max}/K_m
GRPRTSSFAEG-NH_2 (Crosstide)	2.5	38.5	8.4
ARKRERAYSFGHHA-NH_2 (Aktide)	8.8	480	54
ARKRERTYSFGHHA-NH_2 (Aktide-2T)	3.9	230	60

We examined the specificity of these peptides for Akt (Fig. 3-4). These peptides were synthesized following Solid-phase peptide synthesis (SPPS) protocol. These synthesized peptides were reacted with Protein kinase A (PKA), Akt1, PKCα and Rho associated coiled-coil kinase (ROCK) at each optimal reaction condition, respectively. The phosphorylation ratio was measured by Matrix Assisted Laser Desorption/Ionization (MALDI-TOF-MS) and calculated by the following formula:

$$\text{Phosphorylation ratio } \% = \frac{\text{Area of phosphorylated peptide peak}}{\text{Area of peptide peak} + \text{Area of phosphorylated peptide peak}}$$

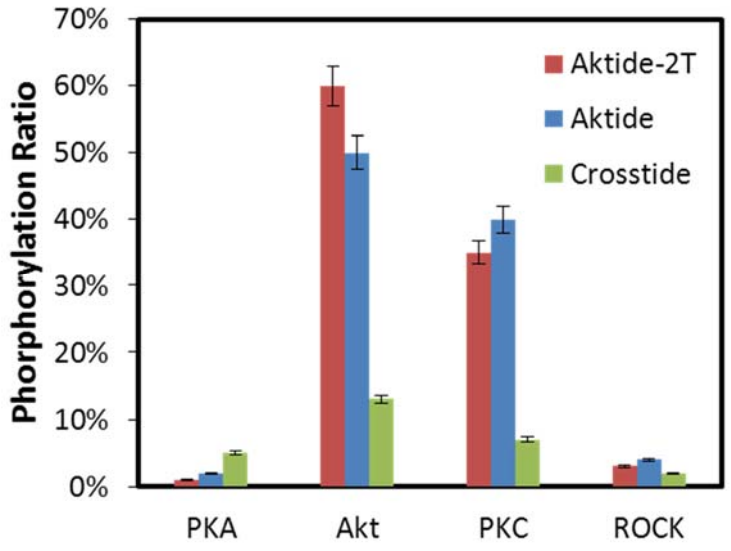

Figure 3-4: phosphorylation ratio of peptides

The phosphorylation result was shown in Fig. 3-4. All of these three peptides showed negligible phosphorylation with PKA or ROCK but they showed low specificity for Akt1 relative to PKCα. Comparing with Aktide, Aktide-2T showed higher specificity for Akt1 relative to PKCα. Thus, Aktide-2T was finally chosen as our Akt specific substrate.

3-3-2 Balance of the cationic densities and endosomal escape moieties

In the chap 2, we designed the polymer using grafted peptide as cationic motif. This was to enlarge the change of the net cationic charges while phosphorylated. But the DNA condensation ability and the cellular uptake seem to be low. This may limit the transfection efficiency as gene carrier. To optimize the balance of cellular uptake and buffering capacity, four polymers with different histidine modification ratio of 25%, 50%, 75% and 100% without peptide was synthesized (data not shown) and named PH22, PH44, PH70, PH94, respectively.

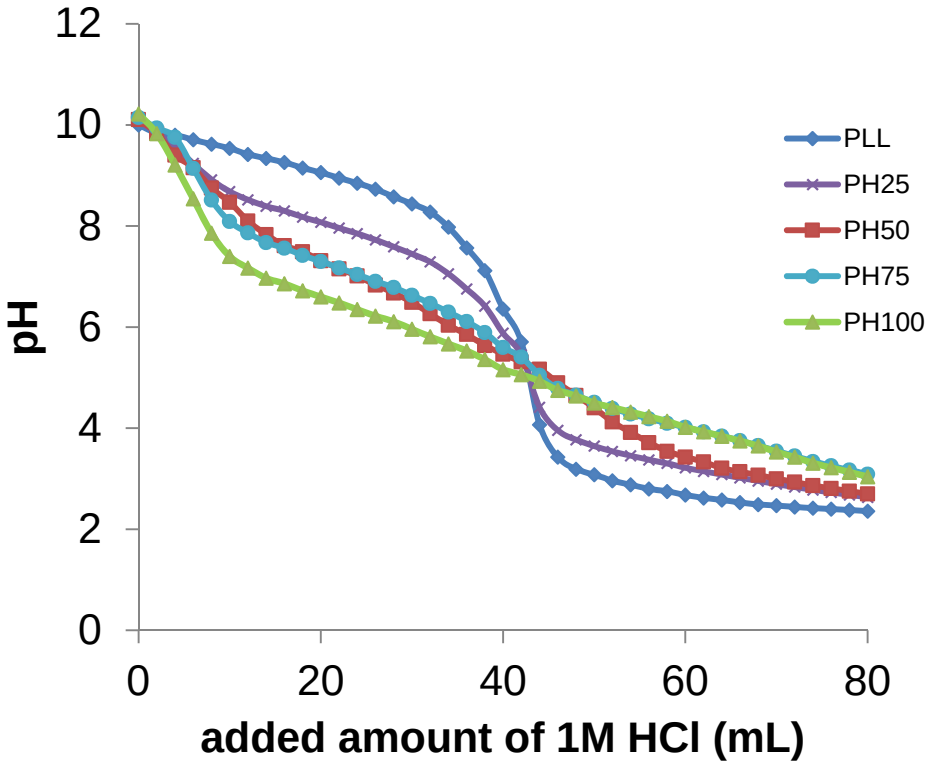

Figure 3-5. pH titration of polymers. Each polymer was dissolved in 2.0 mL of 150 mM NaCl to a final concentration of 0.1 M in monomer units. After adjusting to pH 10, the solution was titrated with 1.0 M HCl to the desired pH.

The buffering capacity of these polymers was evaluated by acid titration in 150 mM aqueous NaCl solution (Figure 3-5). The titration curve of PLL trend turns nearly vertical at neutral pH, suggesting little buffering capacity, while the PH100 showed considerable buffer capacity over almost the entire pH. In the case of histidine partly modified polymers (PH22, PH44 and PH70), the titration curve gives the basic buffering capacity at basic and endosomal pH regions based on PLL and histidine motifs, respectively. Comparing with the weak buffering capacity of PH22, PH44 and PH70 showed similar buffering capacity to PH94. These results indicate that the histidine partly modified PLL retains the complexation and compaction ability

associated with PLL, but also induces endosomal protonation of histidine residues.

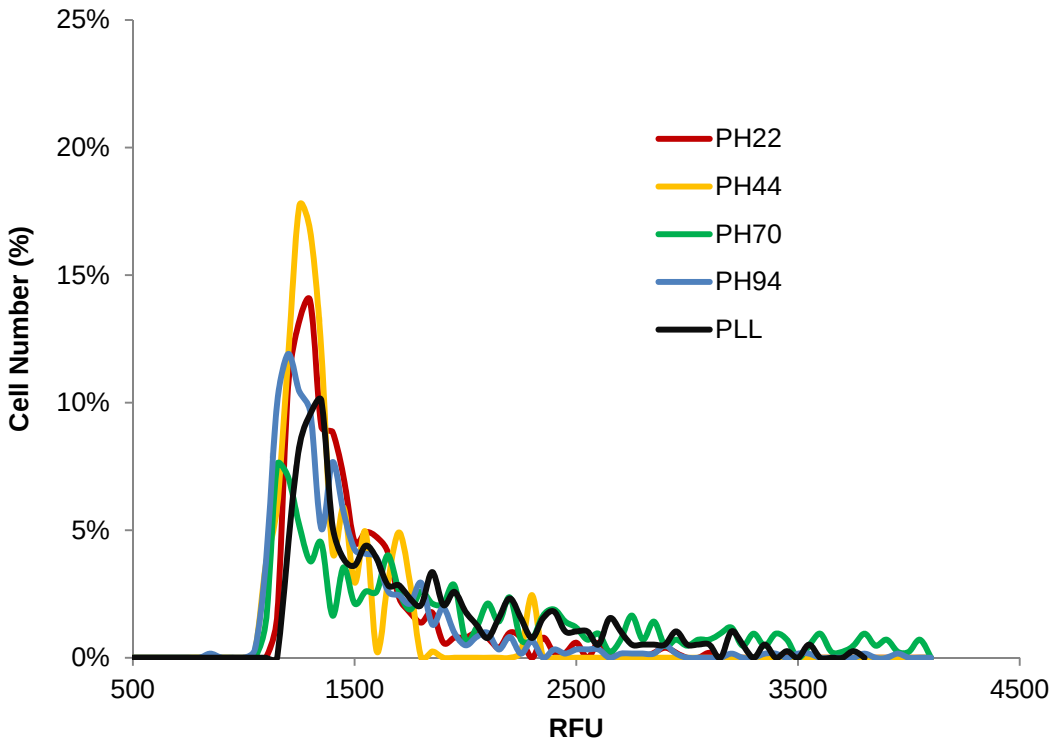

Figure 3-6: Cellular uptake of different polymers in U87MG cell line at N/P = 10.

The cellular uptake of the polyplex was evaluated by using pDNA labeled with YOYO-1 in U87MG cell line. Polymers were prepared at an N/P ratio (the ratios of moles of the amine groups and imidazole groups of polymers to those of the phosphate ones of pDNA) of 10 in Opti-MEM (pH 7.4). As shown in Fig. 3-6, the PH70 and PH94 showed low cellular uptake ability, which probably due to the weak DNA condensation ability of the polymer main chain. Considering the buffering capacity and uptake efficiency, a 50 mol% histidine modification ratio was determined as an optimal balance.

3-3-3 Synthesis of Akt-responsive polymer

The polymer synthesis is following the procedure described in Chap. 2-2-1. The sequence of peptide used here was ARKRERTYSFGHHA-NH_2, the Akt specific substrate which is called Aktide-2T. Since this peptide contains five cationic amino acids and one anionic amino acid, it should have +3 positive charges at neutral pH. Three kinds of polymers were synthesized with different histidine modification ratios of about 0%, 50% and 100%. Their negative control polymers with a peptide sequence of ARKRERTYAFGHHA-NH_2, in which the serine was substituted with alanine, were also synthesized. The ID, peptide and histidine content of the synthesized polymers are summarized in Tab. 3-2. Content of each component was calculated from the ^{1}H NMR spectral signals (Figure 3-7) at δ = 7.57 ppm and δ = 6.79 ppm (the imidazole moiety in the histidine), δ = 7.23 ppm (the benzene moiety in the peptide phenylalanine), δ = 6.60 ppm (the benzene moiety in the peptide tyrosine) and δ = 4.14 ppm (the α-CH moiety in the PLL main chain).

Table 3-2: Histidine and peptide content in the synthesized polymers

ID	Histidine content (mol%)	Peptide content (mol%)	Peptide grafting number/chain
PLL-Akti(S)	-	5.35	2.2
PLL-Akti(S)-His_{50}	49.3	2.68	2.5
PLL-Akti(S)-His_{100}	91.2	8.2	4.7
PLL-Akti(A)	-	6.34	
PLL-Akti(A)-His_{50}	55.1	3.23	3.8
PLL-Akti(A)-His_{100}	80.1	5.48	-
PH22	22.1	-	-
PH44	44.2	-	-
PH70	69.8	-	-
PH94	94.3	-	-

(a)

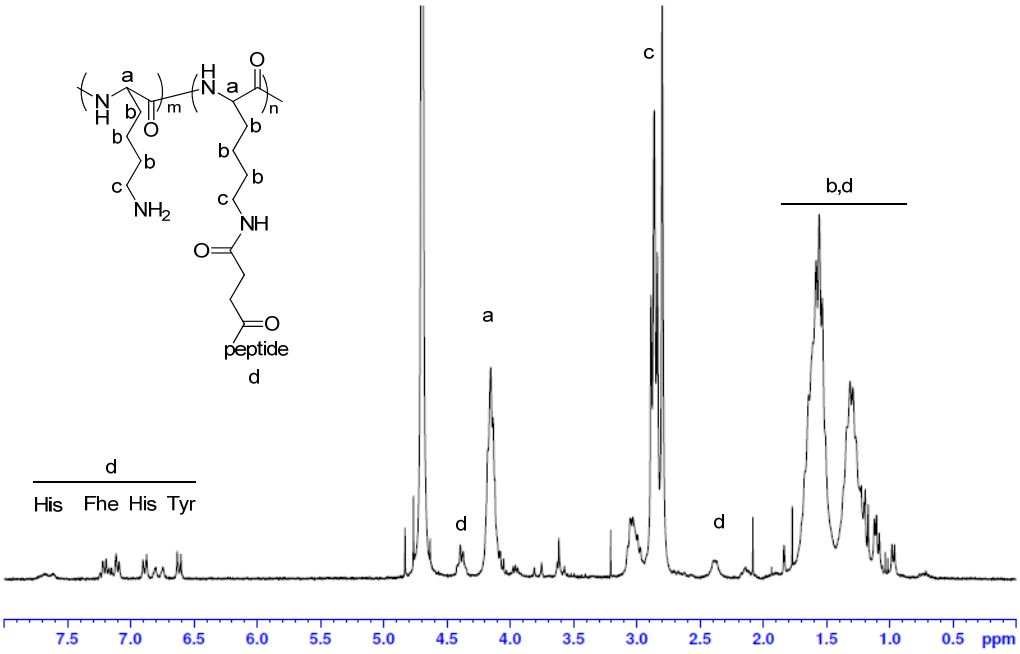
c
b,d
a
d
His Fhe His Tyr
d
d
peptide
7.5 7.0 6.5 6.0 5.5 5.0 4.5 4.0 3.5 3.0 2.5 2.0 1.5 1.0 0.5 ppm

(b)

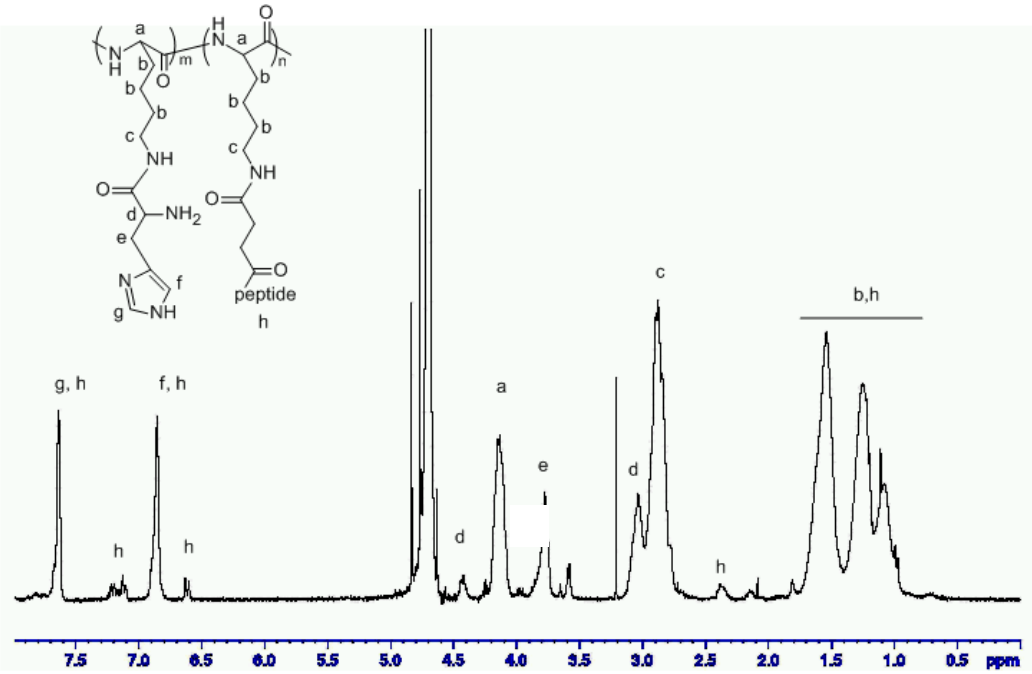
peptide
h
c
b,h
g, h
f, h
a
e
d
h
h
d
h
7.5 7.0 6.5 6.0 5.5 5.0 4.5 4.0 3.5 3.0 2.5 2.0 1.5 1.0 0.5 ppm

(c)

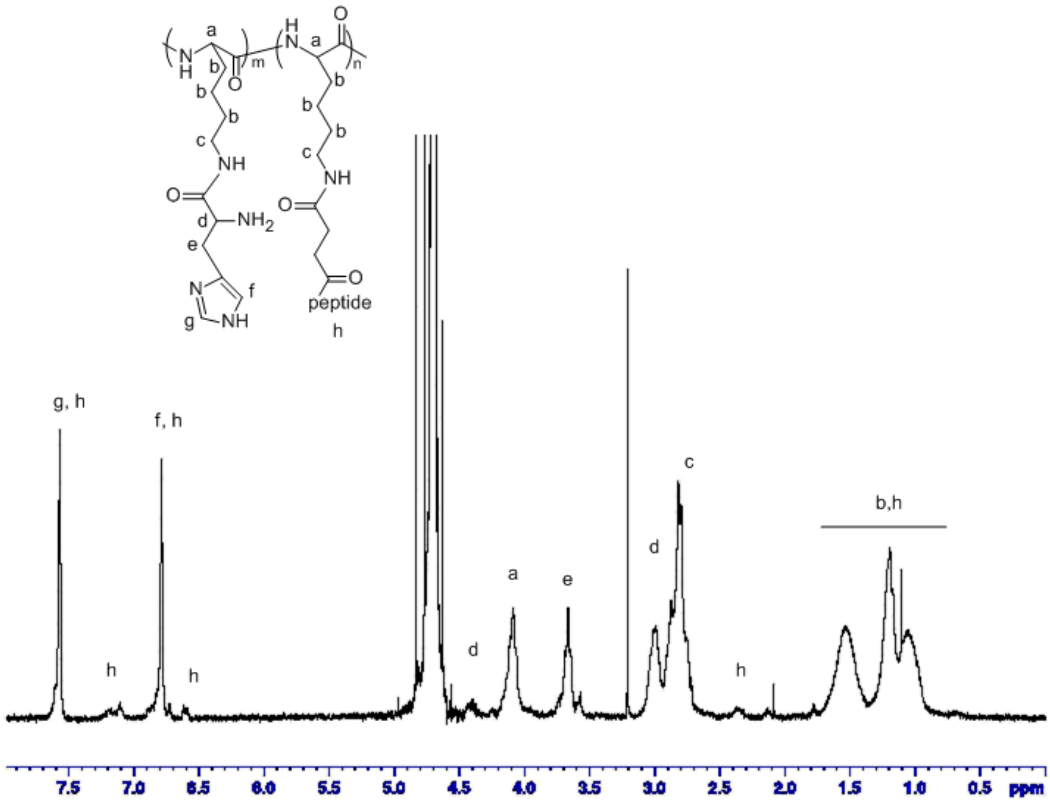

Figure 3-7. ^{1}H-NMR spectrum of (a) PLL-Akti(S), (b) PLL-Akti(S)-His$_{50}$ and (c) PLL-Akti(S)-His$_{100}$ in D_2O

3-3-4 Coupled Enzyme Assay

To check whether these polymers could be phosphorylated by activated Akt, the phosphorylation reaction of polyplex was monitored by coupled enzyme assay(Fig. 3-8). This assay is based on a reaction in which the regeneration of hydrolyzed ATP is coupled to the oxidation of NADH. Along with the phosphorylation reaction by kinase, the ADP generated in this reaction is converted back to the ATP with phosphoenolpyruvate convering to pyruvate by pyruvate kinase. The pyruvate is subsequently converted to lactate by lactate dehydrogenase resulting in the oxidation of one NADH molecule. The reaction level of kinase is

therefor indirectly measured by the rate of NADH absorbance decrease at 340 nm(Fig. 3-8(a)).

After the formation of copolymer/pDNA complexes at an N/P = 4, the phosphorylation reaction of each complex by Akt1 was determined by measurement of NADH absorbance[20, 21]. As shown in Fig. 3-8(b), the negative control polymer PLL-Akti(A)-His_{50} showed no NADH absorbance decrease, which indicate that it cannot be phosphorylated by Akt1. On the other hand, the other three polymers showed a similar time course in the decrease in A_{340}. These results indicate that these polymers could work as Akt1 substrate, and the histidine modification ratio does not affect this phosphorylation.

(a)

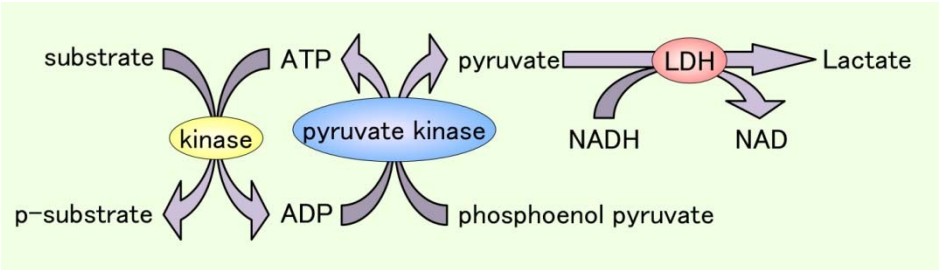

(b)

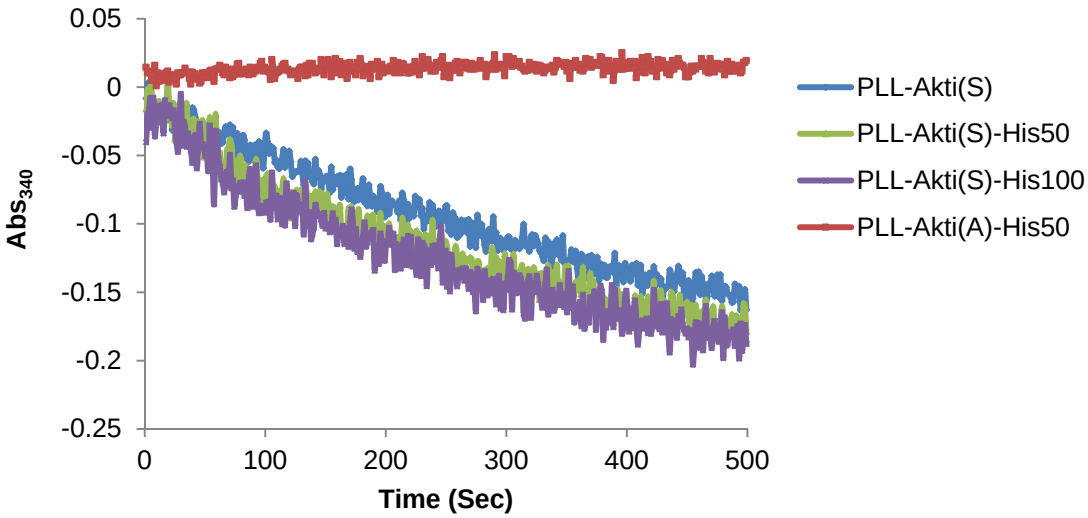

Figure 3-8: (a) principle of coupled enzyme assay and (b) the phosphorylation of polymers by Akt1.

3-3-5 Characterization of the polyplexes

The particle size of polyplexes was determined by dynamic laser light scattering. The polymer/DNA polyplex particles were formed by mixing the polymers and DNA at each N/P ratios. The size and ζ–potential rusules are shown in Fig. 3-9.

As shown in Fig. 3-9(a), at neutral pH, nearly all the polymers gave large size aggregates (> 4 μm) at around N/P ratio = 1 excepting PLL-Akti(A)-His_{50} because of the neutral surface charges of the polyplexes. And at a higher ratio of N/P = 8, the histidine partly modified polymer (PLL-Akti(S)-His_{50} and PLL-Akti(A)-His_{50}) showed higher DNA condensation ability comparing with histidine completely modified one (PLL-Akti(A)-His_{100}). This result indicated the contribution of PLL main chain for DNA condensation. At lower pH (pH = 6.5, Fig. 3-9(b)), all these polymers can condense DNA and form sable polyplex, even in the histidine unmodified one (PLL-Akti(S)). This is due to the peptide sequence, ARKRERTYSFGHHA-NH_2，also contain two histidine residues and showed higher cationic charge at this pH.

(a)

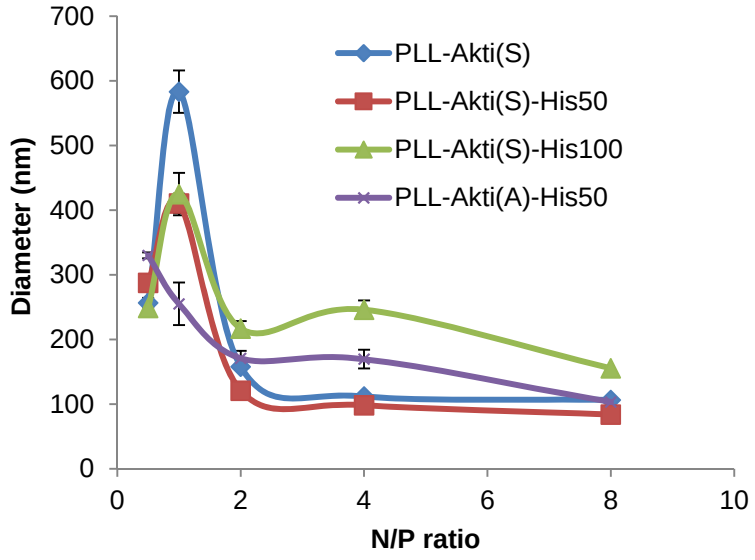
700
600
500
400
300
200
100
0
Diameter (nm)
0
2
4
6
8
10
N/P ratio
PLL-Akti(S)
PLL-Akti(S)-His50
PLL-Akti(S)-His100
PLL-Akti(A)-His50

(b)

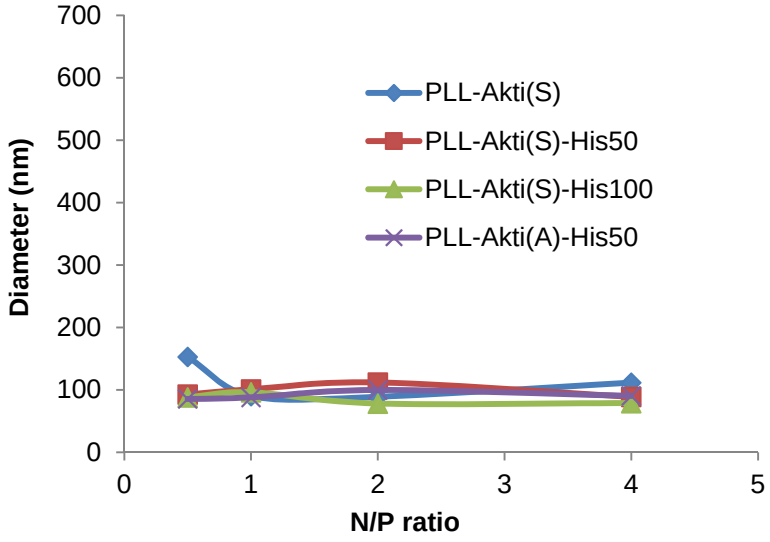
700
600
500
400
300
200
100
0
Diameter (nm)
0
1
2
3
4
5
N/P ratio
PLL-Akti(S)
PLL-Akti(S)-His50
PLL-Akti(S)-His100
PLL-Akti(A)-His50

(c)

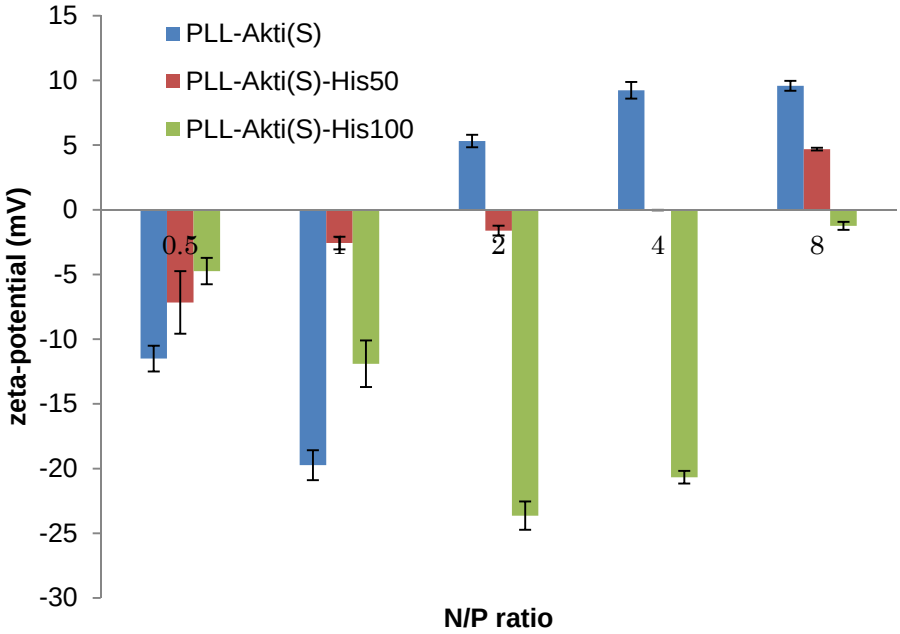

(d)

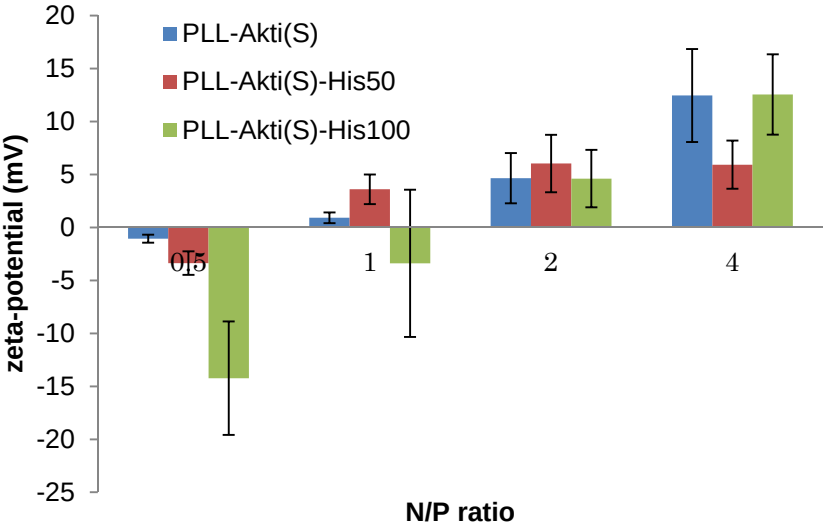

Figure 3-9: Dynamic Laser Light Scattering results of (a) polyplex diameter in 10 mM HEPES buffer (pH = 7.4); (b) polyplex diameter in 10 mM HEPES buffer (pH = 6.5); (c) polyplex ζ-potential in 10 mM HEPES buffer (pH = 7.4) and (d) polyplex ζ-potential in 10 mM HEPES buffer (pH = 6.5). Data are means ± SD of three experiments.

As shown in Fig. 3-9(c), the polyplex formed from PLL-Akti(S)-His100 showed negative surface charge at each N/P ratio, indicating that it cannot form stable polyplex at pH 7.4. All these polymers formed sable polyplex at N/P = 2 at lower pH (pH = 7.4, Fig. 3-9(d)), indicating the better DNA condensation ability of these polymers at pH 6.5.

3-3-6 Ethidium bromide Exclusion Assay

The polyplex formation was also examined by the ethidium bromide exclusion assay. In this plot, each histidine residue was treated as two charges. As shown in Fig. 3-10(a), the RFI leveled off until an N/P ratio reached to around 4. PLL-Akti(S)-His_{50} and PLL-Akti(A)-His_{50} have nearly the same RFI, with is quite similar as PLL. Comparing with these two polymers, PLL-Akti(S)-His_{100} showed much higher RFI, which means it condenses pDNA to a lesser extent than the partly modified polymers. In contrast, at pH 6.5 (Figure 3-10 (b)), all these polymers showed a similar condensation ability as PLL. This is consistent with the results of polyplex diameter and ζ-potential results (Figure 3-9), which reveal that the histidine is much more protonated at pH 6.5 than at pH 7.4.

(a)

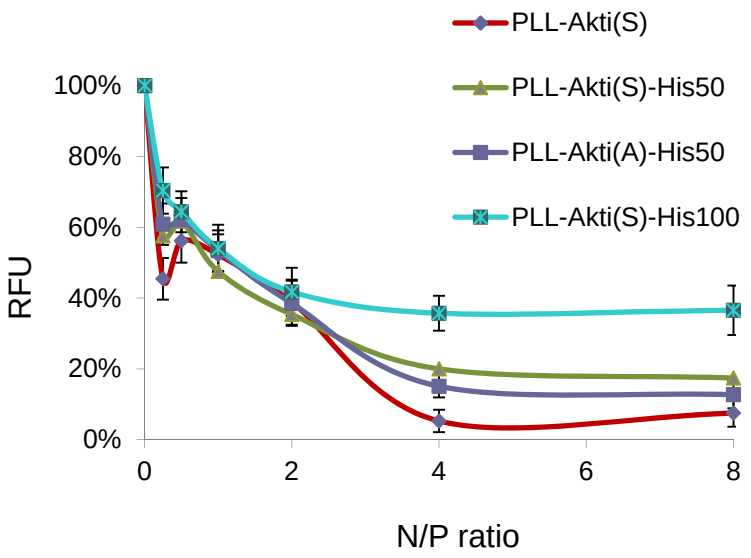

(b)

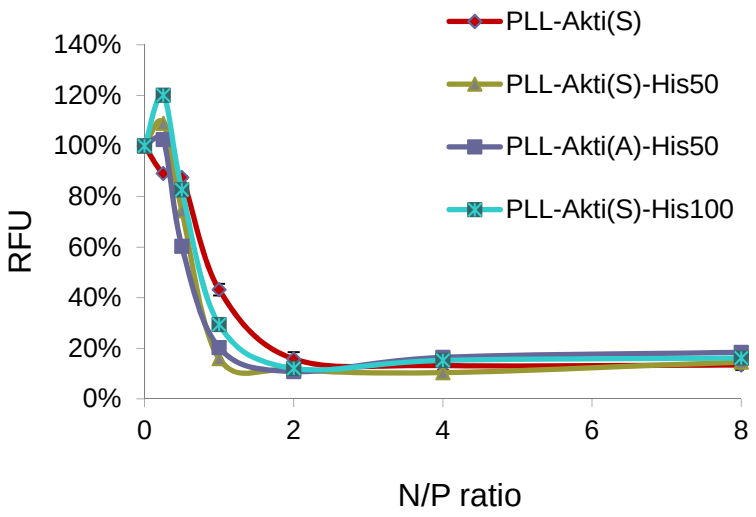

Figure 3-10: Ability of the polymers to condense pDNA at (a) pH 7.4 versus pH 6.5, and (b) in 10 mM HEPES buffer. RFI is the relative fluorescence intensity. N is the total number of amine groups in the polymers (from the peptide lysine, and the main chain lysine and histidine). Each histidine residue was treated as two charges. Data are means ± SD of three experiments.

3-3-7 *In vitro* transfection

Gene expression levels in *in viro* transfection by using these polymers were evaluated by using luciferase encoding pDNA in U87-MG glioma cell lines, in which the Akt is hyper-activated[22]. As shown in Fig. 3-11, the PLL-Akti(S)-His_{50} showed much higher gene expression level than PLL-Akti(A)-His_{50} at N/P = 5 and 10. This result showed that the polyplexes of PLL-Akti(S)-His_{50} responded to Akt to release pDNA for the gene expression. The highest S/A gene expression ratio was obtained at the N/P ratio of 5, where 20 times higher gene expression was observed in PLL-Akti(S)-His_{50} than PLL-Akti(A)-His_{50}. Furthermore, at N/P ratios of 5 to 40, PLL-Akti(S)-His_{100} showed much higher expression level comparing with PLL-Akti(A)-His_{50} and PLL-Akti(S). This result clearly showed a improvement of gene expression by the optimal balance of buffering motif and cationic charge center.

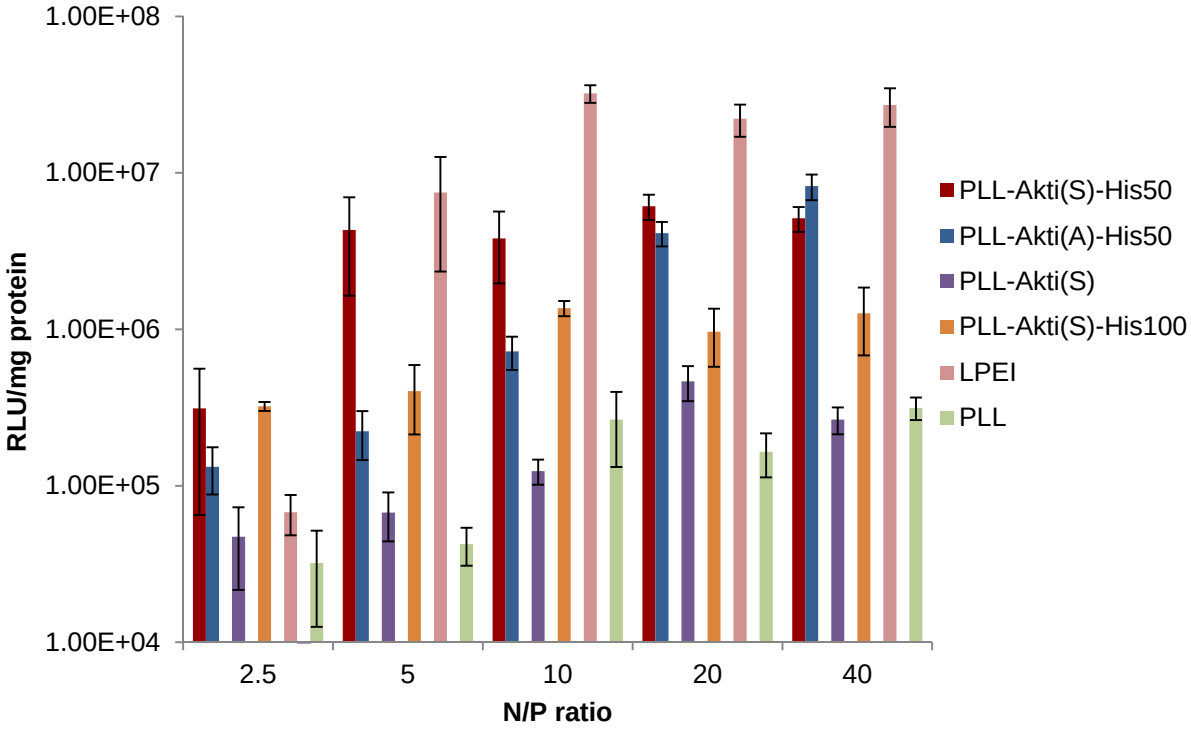

Figure 3-11: Transfection of polyplexes into U87MG cell lines at various N/P ratios.

Data are means ± SD of three experiments.

3-3-8 Influence of the Akt activity on gene expression

The Aktide-2T grafted PLL is supposed to release DNA responding to the hyper-activated Akt from Fig. 3-11. But as shown in Fig. 3-4, this substrate peptide shows relatively low specificity for Akt1 against PKC_{α}. Moreover, both PKC_{α} and Akt are hyper-activated in U87MG cell line. Therefore, obtained liciferase expression may be affected by hyper-activated PKCα. To checkout this possibility, we performed the transfection experiment in the presence of LY294002, a PI3K inhibitor, which can block the activation of Akt indirectly[23-25]. Thus, U87MG cells were cultured with or without 50 μM LY294002 and transfected using the polyplex at N/P = 5. As shown in Fig. 3-12, in the presence of LY294002, the gene expression by PLL-Akti(S)-His_{50} was greatly suppressed, while the PLL-Akti(A)-His_{50} showed no significant difference. This result clearly indicates the Akt-responsive gene expression caused by PLL-Akti(S)-His_{50}.

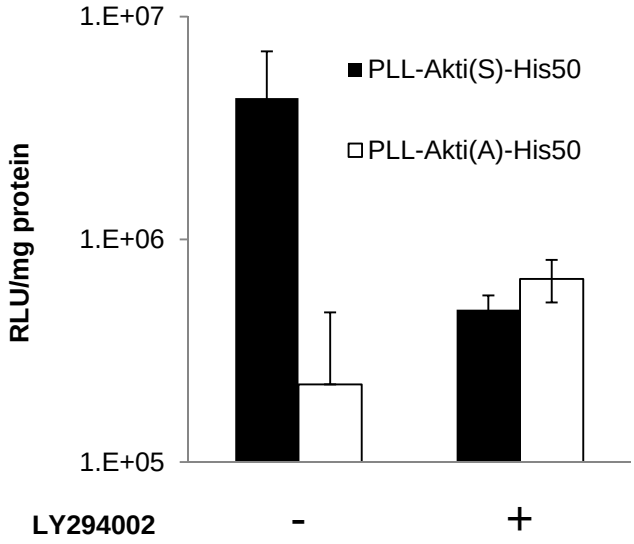

Figure 3-12: Transfection of polyplexes into U87MG cell lines at N/P = 5 with or without 50 μM LY294002.

3-4 Conclusion

In this chapter, we focused on cancer specific gene expression responding to hyper-activated Akt. To overcome the disadvantage of low gene transfection, we reduced the histidine modification ratio and measured the property of the newly synthesized polymer. This polymer showed a slightly lower buffering capacity than the histidine completely modified type, but much higher DNA condense ability and gene transfection level. The Akt responding gene expression was also succeed in U87MG cell line, in which the Akt is hyper-activated.

3-5 Experiment Methods

Synthesis of Akt–specific substrate peptide

The protecded peptides were synthesized by the solid-phase method using the Sieber Amide resin (Merck, Hohenbrunn, Germany) (0.69 mmol/g). In the condensation reaction, the n-terminal protected amino acid (4 eq.)、HOBt·H_2O (4 eq.) 、HBTU (4 eq.) 、DIPEA (8 eq.) was mixed in DMF, and reacted at r.t. for 10 min. The end of each reaction was confirmed by Kaiser Test. After the condensation of the last amino acid, the N-terminus of the peptide was reacted with succinic anhydride in 0.9 M DIPEA/NMP. The peptide was then cleaved from the resin with the remaining protective groups by treating with 1% TFA in DCM solution, and the resulting solution was neutralized by 10% pyridine in methanol. The obtained protected peptide was reprecipitated using cold water and then dried in vacuo. The target peptide was confirmed by MALDI-TOF-MS (Bruker JapanCo., ltd., Tokyo, Japan) without deprotection. The purity of the protected peptides was determined by high-performance liquid chromatography (HPLC).

Synthesis of polymer

The polymer modification reaction was carried out in DMSO directly. PLL·HBr was dissolved in 500 μL DMSO. Then, the protected peptide (30 mg; 6.4 μmol) dissolved in 2.5 mL DMSO was added to the PLL solution, following which HBTU (2.5 mg; 6.4 μmol) and HOBt (0.9 mg; 6.4 μmol) were added as coupling reagents. To this solution, 80 μL of DIEPA was added to adjust the pH from 9 to 10. After reacting for 2 days, Fmoc-His (Trt)-OH, HBTU, and HOBt were added at each plot ratio to further modify

the rest of the amine groups on the PLL.

The resulting polymer was reprecipitated in cold acetyl acetate, and then the Fmoc group was deprotected by adding 20% PPD in DMF. After 10 min, the polymer was precipitated again in cold acetyl acetate. The remainder of the protecting groups were removed by dissolving the polymer in a mixture of 95% trifluoroacetic acid, 2.5% triisopropylsilane, and 2.5% water. After 2 h, the polymer was purified by reprecipitation with cold acetyl acetate three times. The obtained white powder was dissolved and dialyzed against distilled water for 3 days in a semi-permeable membrane bag with a molecular weight cutoff of 3,000 Da. After lyophilization, the final product was obtained as a white powder. The content of the peptide and histidine in the polymer was estimated by ^{1}H NMR spectrum in D_2O using a 300 MHz spectrometer.

Polyplex formation

To prepare polyplexes at various N/P ratios (the ratios of moles of the amine groups and imidazole groups of polymers to those of the phosphate ones of pDNA), 25 μL of 0.1 mg/mL pDNA (pCMV-luc2) and 25 μL polymer solution were diluted by adding 475 μL of 10 mM HEPES (pH 7.4), following which the resulting solutions were mixed and then incubated at room temperature for 30 min. The polyplex diameter and ζ-potential were measured by a Zetasizer (Malvern Instruments, Worcestershire, UK) with a He/Ne laser at a detection angle of 173° at 25 °C.

Coupled Enzyme Assay

Polyplex was formed at N/P = 5 with a peptide motif concentration of 30 μM. After stabilized for 30 min、the final solution containing 30 μM peptide motif、10 mM HEPES

(pH 7.4)、1 mM phosphoenol pyruvate、300 μM NADH、200 μM adenosine-5'-triphosphate (ATP)、1 mM MgCl2、4 U/μl pyruvate kinase、10 U/μl lactate dehydrogenase (LDH) and 2.0 μg/ml Akt1. the decrease rate of NADH absorbance was measured at 340 nm using UV/Vis spectrometer (UV-2550; Shimadzu, Tokyo, Japan).

Ability of polymers to condense DNA at different pH

To check the ability of the polymers to condense DNA, 5 μL of 0.1 mg/mL plasmid DNA was mixed with 1.5 μL of 0.1 mg/mL EtBr. After incubating this mixture for 10 min, 5 μL polymer solution at each N/P ratio was added and the total volume of solution was diluted to 100 μL by adding 10 mM HEPES. After 30 min, its fluorescence intensity was measured by multi-label counter ARVO (Wallac Incorporated, Turku, Finland) (λ_{ex} = 530 nm, λ_{em} = 590 nm, 20 s). The relative fluorescence intensity (RFI) was determined using the following equation: RFI = $(F_{sample}-F_e)/(F_0-F_e)$, where F_{sample}, F_e, and F_0 are the fluorescence intensities of the polyplex, background, and free pDNA without carrier, respectively.

pH titration

Each polymer (0.1 M in repeating unit of backbone polymer) was dissolved in 2.0 mL of 150 mM NaCl. After adjusting to pH 10 with 1.0 M NaOH, the solution was titrated with 80 μL of 1.0 M HCl to the desired pH, which was monitored by AUT-701 (TOA-DKK, Japan).

Cell culture

U87MG cells were cultured in MEM containing 10% fetal bovine serum (FBS), 100

U/mL penicillin, 100 μg/mL streptomycin and 0.25 μg/mL amphotericin B (all from Gibco Life Technologies, Grand Island, NY, USA) under a humidified atmosphere containing 5% CO_2 and 95% air at 37 °C.

Transfection study

pDNA coding luciferase (pCMV-Luc2) was used for transfection. U87MG cells were respectively plated in MEM containing 10% FBS, at a density of 2×10^4 cells/well in a 48-well plate, and then incubated for 24 h. Polyplexes were prepared by mixing pDNA (1 μg) with a polymer at each N/P ratio and incubating for 30 min at room temperature. Just before the transfection procedure, the culturing medium was exchanged for Opti-MEM without serum. Polyplex solution was added, and the cells were incubated for 4 h at 37 °C, 5% CO_2. The solution of polyplex and Opti-MEM was then replaced with 500 μL of fresh culturing medium containing 10% FBS, and the cells were further incubated at 37 °C, 5% CO_2 for 24 h. The cells were washed with PBS and lysed for 20 min with 100 μL of lysis buffer (20 mM Tris-HCl containing 0.05% TritonX-100 and 2 mM EDTA (pH 7.5)). The 10 μL of lysate were mixed with 40 μL of luciferase assay solution (Promega), following which the luminescence of the mixture was measured with a luminometer.

In the Akt activity suppression study, LY294002 at a final concentration of 50 μM was added to the MEM and opti-MEM. Other condition was the same as transfection experiment.

3-6 Reference

1. S.P. Staal, *Proc. Natl. Acad. Sci. U. S. A.*, **1987**, 84, 5034

2. P.F. Jones, T. Jakubowicz, F.J. Pitossi, F. Maurer, B.A. Hemmings, *Proc. Natl. Acad. Sci. U. S. A.*, **1991**, 4171

3. B. Vanhaesebroeck, D.R. Alessi, *Biochem. J.*, **2000**, 346, 561

4. Michelle M. Hill, Brian A. *Hemmings, Phar. & Ther.*, **2002**, 93, 243

5. Masahito Hanada, Jianhua Feng, Brian A Hemmings, *Biochimica et Biophysica Acta (BBA) - Proteins and Proteomics*, **2004**, 1697, 3

6. P.F. Jones, T. Jakubowicz, B.A. Hemmings, *Cell Regul.*, **1991**, 2, pp. 1001

7. D. Brodbeck, M.M. Hill, B.A. Hemmings, *J. Biol. Chem.*, **2001**, 276, 29550

8. D.P. Brazil, B.A. Hemmings, *Trends Biochem. Sci.*, **2001**, 26 657

9. Ingeborg Hers, Emma E. Vincent, Jeremy M. Tavaré, *Cellular Signalling,* **2011**, 23, 1515

10. Ipsita Pal and Mahitosh Mandal, *Acta Phar. Sinica* **2012**, 33, 1441

11. Izuishi K., Kato K., Ogura T., Kinoshita T., Esumi H., *Cancer Res.*,2000, 60, 6201

12. Brognard J., Clark A. S., Ni Y., Dennis P. A., *Cancer Res.*, 2001, 61, 3986

13. Ipsita Pal and Mahitosh Mandal, *Acta Pharmacologica Sinica* **2012**, 33, 1441

14. Kiyotaka Nishikawa, Alex Toker, Franz-Josef Johannes, Zhou Songyang and Lewis C. Cantley, *J. Biol. Chem.*, **1997**, 272, 952

15. Toshiyuki Obata, Michael B. Yaffe, German G. Leparc, Elizabeth T. Piro, Hiroshi Maegawa, Atsunori Kashiwagi, Ryuichi Kikkawa and Lewis C. Cantley, *J. Biol. Chem.*, **2000**, 275, 36108

16. Dario R. Alessi, F. Barry Caudwell, Mirjana Andjelkovic, Brian A. Hemmings,

Philip Cohen, *FEBS Lett.*, **1996**, 399, 333

17. Tung O. Chan, Susan E. Rittenhouse, and Philip N. Tsichlis, *Annu. Rev. Biochem.*, **1999**, 68, 965

18. Roger Meier, Dario R. Alessi, Peter Cron, Mirjana Andjelković and Brian A. Hemmings, *J. Biol. Chem.*, **1997**, 272, 30491

19. Briony E. Cristiano, Joanna C. Chan, Katherine M. Hannan, et al. *Cancer Res.*, **2006**, 66, 11718

20. Riki Toita, Jeong-Hun Kang, Jong-Hwan Kim, Tetsuro Tomiyama, Takeshi Mori, Takuro Niidome, Byungdug Jun, Yoshiki Katayama, *J. Control. Release*, **2009**, 139, 133

21. Y. Katayama, T. Sonoda, M. Maeda, *Macromolecules* **2001**, 34, 8569

22. Ying Li, Donald Dowbenko, and Laurence A. Lasky, *J. Biological Chem.*, **2002**, 277, 11352

23. Giuseppe Viglietto, Maria Letizia Motti, Paola Bruni, Rosa Marina Melillo, Amelia D'Alessio, Daniela Califano, Floriana Vinci, Gennaro Chiappetta, Philip Tsichlis, Alfonso Bellacosa, Alfredo Fusco1 & Massimo Santoro, *Nature Med.*, **2002**, 8, 1136

24. John Brognard, Amy S. Clark, Yucheng Ni, and Phillip A. Dennis, *Can. Res.*, **2001**, 61, 3986

25. A M Martelli, P L Tazzari, G Tabellini, R Bortul, A M Billi, L Manzoli, A Ruggeri, R Conte and L Cocco, *Leukemia*, **2003**, 17, 1974

26. Chris J. Viahos, William F. Matter, Kwan Y. Hui, and Raymond F. Brown, *J.biological Chem.*, **1994**, 269, 5241

27. Stephen P. Davies, Helen Reddy, Matilde Caivano and Philip Cohen, *Biochem. J.*, **2000**, 351, 95

Chapter 4 Conclusion

In this study, we focused on the development of easily-prepared and efficient gene carriers for intracellular signaling responding gene expression. In chapter 2, we developed a PLL-based polymer modified with histidine and PKCα substrate peptide, which can be used as a high efficient and cancer-cell-targeted gene carrier, based on the intracellular signaling – protein kinase Cα. In chapter 3, we focused on Akt responding, which is another disordered protein kinase discovered in many kinds of cancer cells. Furthermore, to enhance the efficiency of this polymer, we reduced the histidine modification ratio and achieved a much higher gene expression level than the previous type.

In chapter 2, PLL was employed as polymer main chain because of its easily modification property. Onto this main chain, almost all the amine groups were modified with histidine to reduce the charge density and introduce the buffering capacity. This design was also intended to increase the charge attenuation during phosphorylation by protein kinase. The rest amine groups of PLL were modified with a cationic PKCα specific substrate peptide. This peptide was intended to work as cationic center for polyplex formation and as phosphorylation reaction center.

These polymeric carriers were synthesized easily by functionalizing the PLL main chain with the protected peptide and histidine, followed by deprotection of the functional groups. The NMR showed that the modification reaction is completely. These polymers could condense pDNA to polyplexes of diameter about 200 nm for cellular uptake. The cationic charge is mainly from the peptide. This polymer showed

buffering capacity at a wide pH range from 8 to 3, which means the modified histidine allowed the polyplexes to effectively escape from the endosome, which is confirmed by confocal microscope. The carriers showed a clear improvement in the PKCα-responsive expression of pDNA in cancer cells. These results indicated that this PLL-based gene carriers could be potentially applicable to cancer cells.

In chapter 3, we tried to overcome a disadvantage of the PLL-based polymer. Histidine fully modified PLL back bone showed no charges at neutral pH. This could be of help of increasing the net charge shift during phosphorylation by protein kinase. But the results showed that the difference of transgene expression between this polymer and its negative control was not so large, about 7 times and 16 times in U87MG and B16 cell line, respectively. Furthermore, this low charge density leads the weak DNA condensation ability at neutral pH, which prohibited the cellular uptake. To overcome this disadvantage, we reduced the histidine modification ratio. As respected in the chapter 2, we applied this polymer to another kinase, Akt.

Aktide-2T was chosen as the Akt specific substrate. This peptide showed the higher value of K_m/V_{max} for Akt1 comparing with Aktide and Crosstide. It also showed best specificity for Akt1 relative to PKA, PKCa and ROCK. 50 mol% hisitidine modified PLL showed a good balance between buffering capacity and DNA condensation ability and was chosen as the polymer back bone. This newly synthesized polymer showed slightly lower buffering capacity than the histidine completely modified type, but much higher DNA condensation ability and gene transfection level. The gene expression level is only about 10 times lower than LPEI 25KDa. The Akt responding was confirmed by coupled enzyme assay, the cancer specific gene expression was also succeed in U87MG

cell line, in which the Akt is hyper-activated. Furthermore, the cationic charge of PLL seems not affect the cell signaling responding gene expression.

In this study, we focused on easily preparation and high efficiency of cancer-specific gene carrier. These results showed that PLL could be a good carrier after proper modification. But there are also a lot of disadvantages of this study, i.e., lack of in vivo stability, weak cancer responding ability and unstable polyplex formation. We wish this study could be a reference in the future study.